Hearing in Two Closely Related *Peromyscus* Species (*Peromyscus maniculatus* and *P. leucopus*)

Luberson Joseph[1], Emily Margaret New[1], Desi Marie Joseph[1], Tamara Chenell Woodley[1], Vanessa Yamileth Franco[1], Ben-Zheng Li[2], Guinevere OU Wogan[1], and Elizabeth A. McCullagh[1*]

[1]Oklahoma State University (OSU), Department of Integrative Biology, College of Arts and Sciences, Stillwater, Oklahoma 74078, USA
[2]University of Colorado Anschutz Medical Campus, Department of Physiology and Biophysics, Aurora, Colorado 80045, USA

*Corresponding author: elizabeth.mccullagh@okstate.edu
501 Life Sciences West, Stillwater, OK 74074 USA

ABSTRACT

The genus *Peromyscus* has been extensively used as a model for ecological, behavioral, and evolutionary investigations. We used auditory brainstem responses (ABRs), craniofacial morphology, and pinna measurements to compare characteristics that impact hearing in two wild-caught species, *P. leucopus P. maniculatus*. We observed significant statistical differences in craniofacial and pinna attributes between species with *P. leucopus* overall exhibiting larger features than *P. maniculatus*. ABR recordings indicated that both species showed similar best frequency thresholds between 8-24 kHz. We found significant effects of intensity on amplitude ratio of wave I and IV for *P. maniculatus*, but not *P. leucopus* and effects of wave number on slope of the latency-intensity function with higher wave IV and shorter wave I slope of latency intensity function in *P. leucopus*. Finally, the data showed significant differences in latency shift of the DN1 component of the BIC in relation to ITD between species, while no significant differences were observed across relative DN1 amplitude. This study supports the used of *P. leucopus* and *P. maniculatus* as future model species for auditory research.

Keywords: binaural hearing, *Peromyscus*, auditory brainstem recordings, hearing, pinna, interaural timing difference (ITD)

INTRODUCTION

Hearing and sound localization are critical for the survival and fitness of all taxa. In small mammals, sound localization facilitates predator avoidance, capturing prey, finding mates, foraging, and conspecific communication (Colburn et al., 1987; Grothe et al., 2010; Kidd et al., 1995). To perceive sound source location, mammals rely on interaural time differences (ITD) (for low frequency sound in the horizontal plane) and interaural level differences (ILD) (for high frequency sound) between the two pinnae. ITD and ILD cues are influenced by the size of the head and the shape of the pinna (Blauert, 1997; Grothe et al., 2010). The auditory brainstem consists of specialized regions that integrate ITD and ILD information from each ear. Despite decades of research on hearing and sound localization in small mammals (Blauert, 1997; Grothe et al., 2010; Heffner, 2001), our understanding of species-specific biological variation in sound localization and their hearing ranges continues to need to be explored (Capshaw et al., 2023).

To understand the mechanism of hearing, animal models, including laboratory and wild rodents, can serve as valuable tools. Most studies have used the laboratory house mouse (*Mus musculus*) as a model in hearing research due to its sensitive hearing, ease to breed and maintenance in laboratory settings, and genetic manipulability (Capshaw et al., 2022; Ehret and Dreyer, 1984). Yet, the limited genomic diversity in inbred laboratory rodents pose challenges to fully recapitulating the broad spectrum of human disorder phenotypes (Voelkl et al., 2020). The house mouse has faced criticism as a model for auditory research, owing to its poor sensitivity to

low frequency sounds, increased vulnerability to noise, and minimal audiometric variation within strains (Capshaw et al., 2022). Moreover, the house mouse has a short lifespan and may not exhibit aging patterns similar to other mammals with long lifespan such as bats, African mole-rats or humans (Dammann, 2017). In hearing studies, there has been relatively limited used of wild rodent models to understand the mechanism of hearing with aging. However, the auditory field has leveraged many alternative species including the Mongolian gerbil (*Meriones unguiculatus*), which is valued for its similarity of hearing range to human (Heeringa et al., 2020; Jüchter et al., 2022; Mills et al., 1990). Although these model taxa have shed insights in understanding the fundamental mechanism of hearing, it is essential to continue to consider comparative approaches that include a wider range of species, particularly those that reflect natural diversity in their vocalization, have long life spans, and vary in habitat use (Capshaw *et al* 2023).

The white-footed mouse (*Peromyscus leucopus*) and the North American deer mouse (*Peromyscus maniculatus*) are two of the most abundant rodents in North America (Kirkland and Layne, 1989). They both belong to the family Cricetidae and are more closely related to hamsters and voles than to mice of the family Muridae. Both species have been extensively studied as model systems in ecological, behavioral, biogeographical, and evolutionary investigations with regard to their physiological adaptation to varying habitat types (arboreal habitats, grassland, woodlands, brushlands, swamps, and desert), their social system (mainly promiscuous), and behaviors (maternal, winter nesting, climbing, and agonistic behaviors) (Bedford and Hoekstra, 2015; Harney and Dueser, 1987; Lewarch and Hoekstra, 2018). Both species are also of human health concern with regards to their carrying viruses and pathogens including hantavirus, leptospirosis, and plague (Childs et al., 1994; Larson et al., 2018).

Recently, members of the genus *Peromyscus* have emerged as valuable model systems in the field of neuroscience for studying age-related hearing loss due to their considerable lifespan compared to mammals of similar size. *Peromyscus* species exhibit an average lifespan nearly double that of *M. musculus,* when reared in laboratory settings, with the potential to live up to eight years (Burger and Gochfeld, 1992; Guo et al., 1993). In addition, *Peromyscus* species hear best between 8 to 16 kHz, as demonstrated by low ABR thresholds, with the ability to hear up to 65 kHz (Capshaw et al., 2022; Dice and Barto, 1952; Ralls, 1967). In comparison to *M. musculus*, *Peromyscus* rodents display lower production of reactive oxygen species and enhanced resistance to oxidative stress, resulting in delayed accumulation of oxidative damage to deoxyribonucleic acid over the *Peromyscus* lifespan (Csiszar et al., 2007; Labinskyy et al., 2009; Shi et al., 2013), among other preventive effects which may slow cochlear aging (Ohlemiller and Frisina, 2008). *Peromyscus* species occupy a large range of habitats, which offer unique opportunities to identify alleles underlying natural variation in biomedically relevant behaviors (Dewey and Dawson, 2001; Vrana et al., 2014). Moreover, both species are phylogenetically closely related (Bradley et al., 2007; Fiset et al., 2015; King, 1968), occur in sympatry, and share diverse morphological similarities such as tail length and pelage color (Millien et al., 2017; Platt et al., 2015) . However, the two species differ in their craniofacial and pinna sizes (Light et al., 2021) which may contribute to differences in their hearing as we know that pinna size impact hearing by enhancing sound collection and amplification, improving frequency discrimination, and facilitating more accurate sound localization (Heffner et al., 2020; Heffner and Heffner, 1982). Therefore, members of the genus *Peromyscus* show promise as models that can be used to complement auditory research across species and consequently can be reference taxa to explore small mammals' hearing across longer lifespans.

The purpose of this investigation is to compare hearing-related anatomy, hearing range, and binaural hearing of *P. leucopus* and *P. maniculatus* measured by craniofacial features, pinna size, and auditory brainstem responses (ABRs). We expect that *P. maniculatus* will have shorter binaural latency compared to *P. leucopus*, due to smaller overall size, pinna, and craniofacial measurements. We also expect that there will be differences in other measures of hearing including best frequency hearing thresholds and monaural ABRs (monaural amplitudes and monaural latencies) due to differences in body size, habitat, and other variability between these two closely related species.

MATERIALS AND METHODS

All procedures used for all experiments complied with the guidelines of the American Society of Mammologists (Sikes et al., 2011), were approved by the Oklahoma State University Institutional Animal Care and Use Committee (IACUC), and permission from an Oklahoma Department of Wildlife Conservation scientific collecting permit.

Animals

Experiments were conducted on 26 individuals, including 15 wild *P. leucopus* (9 males, 6 females) and 11 wild *P. maniculatus* (9 males, 2 females). Animals were live trapped using aluminum Sherman (H.B Sherman Traps, Inc. Tallahassee, FL) non-folding traps (3” x 3” x 10”) between June 2021 and July 2022 at three different locations across Oklahoma, USA (Packsaddle Wildlife Management Area, James Collins Wildlife Management Area, and Payne County) (Figure 1). The traps were baited with old fashioned oats and creamy peanut butter, left overnight, and collected the next morning (~12 hours). Upon capture, animals were aged, morphologically identified to species in the wild according to (Caire, 1989) and confirmed with

122 DNA barcoding polymerase chain reaction (PCR) of collected tail snips. Animals ages were
123 calculated for each species based on body mass and were divided into three age groups (Juvenile,
124 subadult, and adult) (see table 1). Animals were then transported to the laboratory for ABRs.
125

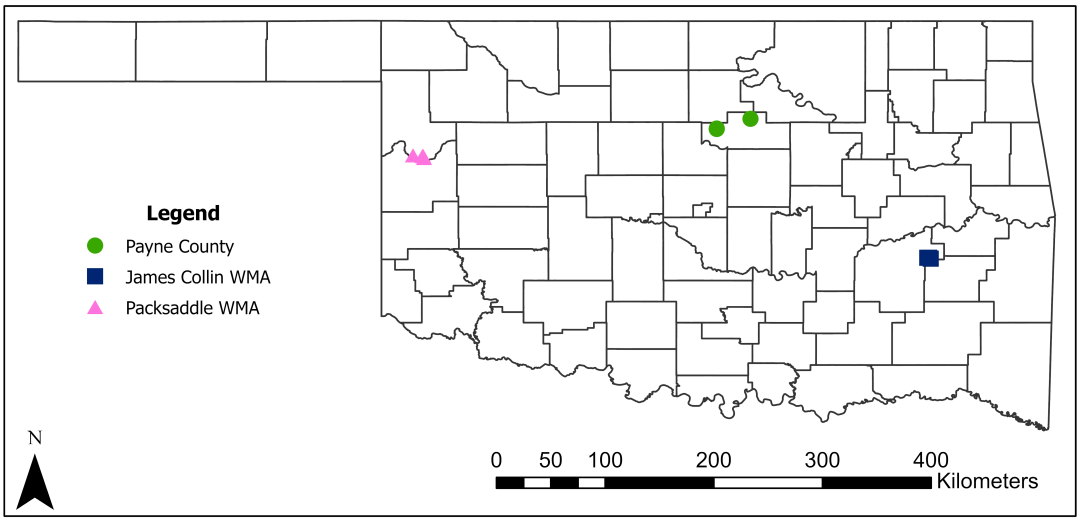

126

127 **Figure 1:** Map showing trapping site locations in Oklahoma. Packsaddle wildlife management area
128 (WMA) sites are represented by pink triangles, James Collin wildlife management area (WMA) sites are
129 represented by blue squares, and Payne County sites are represented by green circles.
130
131
132
133 **DNA extraction, amplification, and sequencing**

134 Deoxyribonucleic acid (DNA) was extracted from tail tissue samples by proteinase K
135 digestion using a Qiagen DNeasy blood and tissue kit (Hilden, Germany) and the protocol
136 outlined by (Nicolas et al., 2012). The DNA concentration and purity were first determined by
137 using a Thermo Scientific Nano-Drop Lite-Spectrophotometer (Fisher Scientific,
138 Spectrophotometer, Nanodrop Lite 6V 18W, Wilmington, DE). The CO1 gene was amplified

using the primer sequences (CCTACTCRGCCATTTTACCTATG) and (ACTTCTGGGTGCCAAAGAATCA) (Ducroz et al., 2001; Robins et al., 2007). DNA samples were assayed in a 50 µl reaction with 25 µl Phusion Master mix, 2.5 µl forward primer, and 2.5 µl reverse primer and mQ water. The PCR comprised of 35 cycles: 95° C for 300 seconds; 30 seconds at 94° C, 40 seconds at 55° C, 90 seconds at 72 ° C, and a final 300 second extension at 72 ° C. The double-stranded PCR products were purified and sequenced at the Center for Genomics and Proteomics of Oklahoma State University (Stillwater, Oklahoma, USA). All sequences were compared with other COI sequences using the NCBI GenBank (Sayers et al., 2022, 2021) databases to confirm species identification (supplemental Figure 1, supplemental Table 1).

Morphological measures

Craniofacial morphology features including pinna size, tail length, body length, and body mass were recorded for each animal using a six-Inch Stainless Steel Electronic Vernier Caliper (DIGI-Science Accumatic digital Caliper Gyros Precision Tools Monsey, New York, USA) and a digital stainless Steel Electronic scale (Weighmax W-2809 90 LB X 0.1 OZ Durable Stainless Steel Digital Postal scale, Chino, California, USA). Measurements of animal head and pinna including inter-pinna distance (mm) (measurement between the two ear canals), nose to pinna distance (mm) (measurement from the tip of the nose to the middle of the pinna), pinna length (mm) (basal notch to tip, excluding hairs), and pinna width (mm) were measured (Figure 3A). Pinna measurements (pinna width and pinna length) were used to calculate the effective pinna diameter which is the square root of the pinna length multiplied by the pinna width (Anbuhl et al., 2017). Tail length (sacrum to caudal tip, excluding hairs), body length (tip of nose to caudal

tip), and weight to the nearest gram were taken for each animal. To assess dependence of morphological traits on body size, log values of traits (pinna width, length etc.) were plotted against the log body length (supplemental Figure 2).

Auditory Brainstem Response (ABR) recordings

We recorded ABRs from wild *P. leucopus* and *P. maniculatus* using similar procedures as previous publications(Chawla and McCullagh, 2022; McCullagh et al., 2020; New et al., 2024). Rodents were sedated with an intraperitoneal injection of 60 mg/kg ketamine and 10 mg/kg xylazine for initial anesthesia followed by maintenance dosage of 25 mg/kg ketamine and 12 mg/kg xylazine. After being fully sedated, as indicated by lack of toe pinch reflex, the animals were transported to a small sound-attenuating chamber (Noise Barriers, Lake Forest, IL, USA), and positioned on a water pump heating pad to maintain a body temperature of 37° C. Subdermal needle electrodes were inserted under the skin at midline between the ears over the brainstem (apex, active electrode), directly behind the apex on the nape (reference), and in the back leg of the sedated animals (ground electrode) for differential recordings. To obtain and amplify evoked potentials from electrodes positioned below the skin of the animal, we used a Tucker-Davis Technologies (TDT, Alachua, FL, USA) RA4LI head stage, a RA16PA preamplifier, and a Multi I/O processor RZ5 attached to a PC with custom Python software to record the data. Data were processed using a second order 50-3000 Hz filter and averaged across 10-12 ms of recording time over 500-1000 repetitions. Acoustic stimuli for frequencies of 32 – 64 kHz were presented to animals using TDT Electrostatic Speakers (TDT EC-1) or TDT Electrostatic Speaker-Coupler Model (TDT MF-1) for frequencies of 1 – 24 kHz and broadband clicks attached through custom ear bars with Etymotic ER-7C probe microphones (Etymotic

Research Inc. Elk Grove, IL) for calibration of sounds in the ears. Ear bars had the ER-7C probe microphones threaded through the tapered end of the tube with the speakers connected through the provided tubing to the front of the tube creating a closed-field presentation of stimuli. Tone stimuli were 4 ms in total duration with a 1 ms on-ramp and 1 ms off-ramp (2 ms ± 1 ms on/off ramps). Click stimuli were 0.1 ms in duration with alternating polarity. Acoustic stimuli were presented to the animal with a 30 ms interstimulus interval with a standard deviation of 5 ms (Laumen et al., 2016a). Randomizing interstimulus interval between each presentation has been shown to optimize the ABR waveform (Wang et al., 2020). Stimuli were produced at a sampling rate of 97656.25 Hz through a TDT RP2.1 real-time processor controlled by a custom Python program.

ABR response threshold

ABR response thresholds were determined by using the visual technique outlined by (Brittan-Powell and Dooling, 2004). In short, threshold was defined to be between the intensity at which the waveforms were no longer present and the previous intensity at which they were visible in 5- and 10-dB increments (5 dB increments were used when near threshold). This method was used for analyzing the audiogram for best hearing frequencies presented (1, 2, 4, 8, 16, 24, 32, 46, 64 kHz) and intensities (90 - 10 dB SPL) in addition to click threshold.

Monaural auditory brainstem response recordings

To generate monaural evoked potentials, broadband click stimuli were presented independently to each ear of the sedated animal. Peak amplitude (voltage from peak to absolute trough) and peak latency (time to peak amplitude) were measured across the four peaks of the

auditory brainstem recording waveforms (Figure 4A, 4B). To calculate the monaural latency and amplitude for each species, we calculated the average of the monaural amplitude or latency of waves I and IV from the ABRs data obtained for sound presentation in each ear across intensities (60-90 dB SPL) (New et al., 2024; Zhou et al., 2006). We next calculated the slope of latency for each individual to demonstrate the effects of click intensity on the peak latency of the ABR waves I and IV following the methods of Zhou et al. (2006). In brief, the slope of each latency intensity function was estimated by taking the change in peak latency and dividing it by the intensity difference of each wave for each animal (Figure 2, Ba, b). The latency slope data was used to make comparisons in monaural peak latency between species.

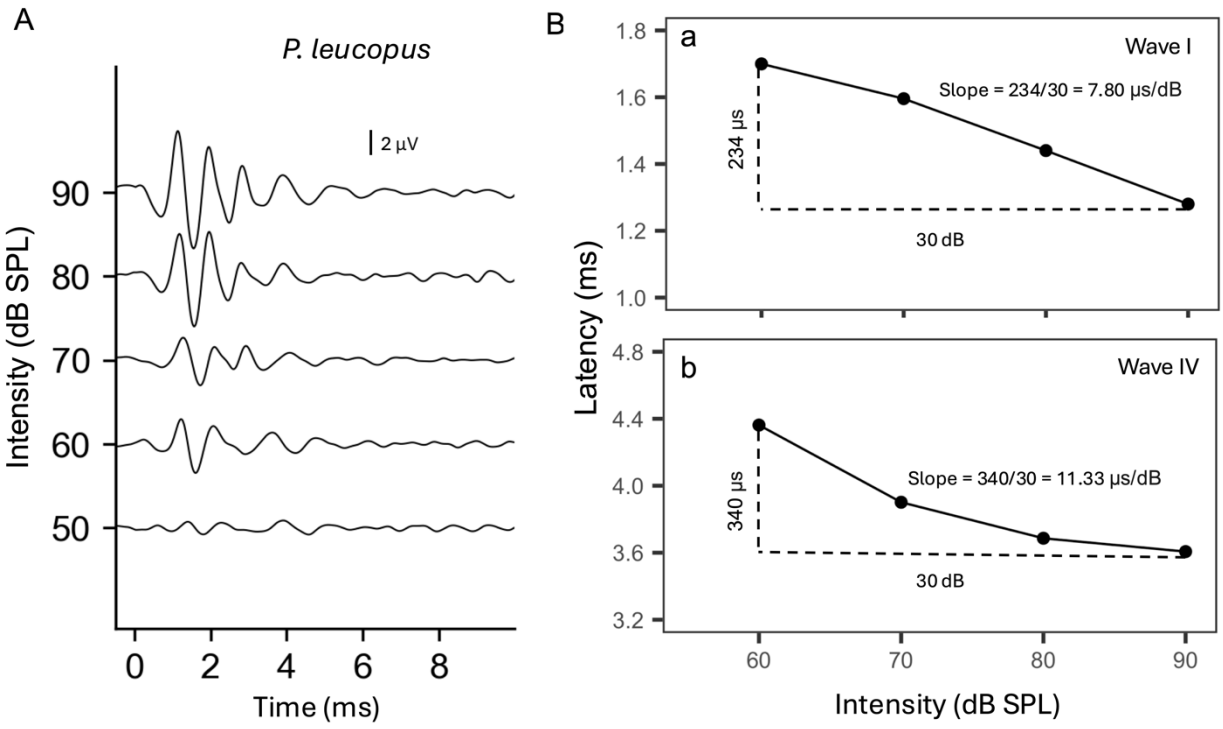

Figure 2: Auditory Brainstem response patterns of a female *P. leucopus* determined with clicks of different intensities. Peak latency of monaural wave I and IV decrease with increasing click intensity (dotted lines). B (a) represents latency intensity functions of wave I and B (b) shows latency intensity functions of wave IV. The slope of the latency intensity function was calculated as the amount of change in peak latency per decibel.

Binaural auditory brainstem response recordings

To produce the binaural ABR response, we simultaneously played broadband click stimuli (same as above) at 90 dB SPL to both pinnae of the sedated animal. The binaural interaction component (BIC) of the ABR was determined by subtracting the sum of the two monaural auditory brainstem evoked responses from the binaural auditory brainstem response recordings (Benichoux et al., 2018; Laumen et al., 2016a). Custom Python software was used to measure the BIC amplitude and latency, with amplitude calculated to the baseline of the recording (Chawla and McCullagh, 2022). BIC was defined as the negative peak wave (DN1) at wave IV of the ABR after subtraction of the summed monaural and binaural responses. To calculate how BIC varies with interaural time difference (ITD), both species were presented with click stimuli that had shifting ITDs of -2.0 to 2.0 ms in 0.5 ms steps. We calculated the peak latency and amplitude of DN1 for each ITD for each species. The ITD latency shift of the DN1 component of the BIC was determined in relation to the latency of DN1 at 0 ITD. The DN1 amplitude is highest at 0 ITD therefore amplitudes for ITD shifts were transformed to relative amplitude with respect to 0 ms ITD to normalize recorded data (Laumen et al., 2016a). The average latency shift and relative DN1 amplitude values were used to make comparison of binaural auditory brainstem responses as function of ITD between species.

Statistical analyses

All analyses and figures were created in R Studio version 4.0.3 (R Core Team 2020), using ggplot2 (Wickham, 2016) and lme4 (Bates et al., 2014) packages. Two-way analysis of variances (ANOVAs) were used to statistically compare morphological characteristics between species. Log-transformed morphological features (pinna width, length, etc.) were compared with log body length and slope of the linear fit to describe potential allometry (slope > 1 indicating positive allometry and < 1 indicating negative allometry). Linear mixed-effects models (LMMs)

were performed on multivariate data (hearing range and ABR amplitudes and latencies) with species, frequency, percentage relative DN1 amplitude, and shifts in DN1 latency of BIC as fixed effects and animal as a random effect. Estimated marginal means were used for pairwise comparisons of frequency, relative amplitude and latency between both studied species (Russell, 2018). To estimate potential effects of body size or species on BIC relative DN1 amplitude and latency of the DN1 component of the BIC relative to ITD at 0, LMMs were performed with fixed effects of species, ITD, and body size and animal as a random effect compared to a null model that excluded body size.

RESULTS

Based on the NCBI GenBank species identification systems for COI, of the tail samples from the 26 animals collected, 15 individuals were identified as *P. leucopus*, and 11 as *P. maniculatus* (supplemental table 1, Figure 1). *P. maniculatus* body length ranged from 55 to 78 millimeters with mean body mass of 12 grams, while *P. leucopus* body length ranged from 65 to 93 millimeters with mean body mass of 21 grams (Table 1).

Species	Age group	Body mass range (g)	Sample size (male, female)
P. maniculatus	Juvenile	< 14	8 (7, 1)
	Subadult	14 – 17	0
	Adult	> 17	3 (2, 1)
P. leucopus	Juvenile	< 13	1 (1,0)
	Subadult	13 – 18	4 (3, 1)
	Adult	> 18	10 (5, 5)

Table 1: Age was estimated based on body mass for each species based on published literature. Ages for *P. maniculatus* was describe as follows: Juveniles < 14 grams, subadults, between 14-17 grams, and adults, > 17 grams (Fairbairn, 1977). We inferred ages for *P. leucopus* as follow: Juveniles < 13 grams, subadults, between 13 – 18 grams, and adults > 18 grams (Cummings and Vessey, 1994). We did not make comparisons by ages due to limited sample sizes by age groups.

Morphological characteristics

Previous studies have shown that *P. leucopus* and *P. maniculatus* have significant differences in pinna sizes and craniofacial features (Choate, 1973; Light et al., 2021; Millien et al., 2017). We observed significant statistical differences for pinna attributes including pinna length (Df = 1, 24; F = 11.79; p = 0.0021), and pinna width (Df = 1, 24; F = 8.47; p = 0.0076) (Figure 3B and 3C respectively). In general, *P. leucopus* had longer and wider pinnae compared to *P. maniculatus*, with mean pinna length and width estimated at 15.30 and 8.02 mm for *P. leucopus* and those of *P. maniculatus* were 13.15 and 6.42 mm, respectively. Similarly, effective pinna diameter (Df = 1, 24; F = 13.69; p = 0.0011) was significantly different between species, with *P. leucopus* having a wider effective pinna diameter compared to *P. maniculatus* (Table 2, Figure 3D). Craniofacial features including inter-pinna distance (Figure 2F; Df = 1, 24; F = 9.08; p = 0.0060) and distance from the nose to the pinna (Figure 3E; Df = 1, 24; F = 5.82; p = 0.0239) were significantly different between species with *P. leucopus* exhibiting a wider distance between pinnae and a longer distance from the nose to the pinna. Like pinnae morphology and craniofacial features, there were significant differences in body mass (Df = 1, 24; F = 24.2; p = 0.00005 , Figure 3I), tail length (Df = 1, 24; F = 25.76, p = 0.0245, Figure 2H), and body length (Df = 1, 24; F = 18.32; p = 0.0002, Figure 3G) between both species, with *P. leucopus* weighing significantly more including longer tails and longer body length than *P. maniculatus* (Table 2). We tested if there were sex differences in craniofacial and pinna sizes in *P. leucopus*. There were no significant differences in craniofacial and pinna sizes between male and female *P. leucopus* (all p-value > 0.05). Sex differences were not explored for *P. maniculatus* due to limited number of female subjects of this species (9 males, 2 females). When anatomical data were compared for potential effects of body size (allometry), log features (pinna width, etc.) compared to log body

294 length did not show positive allometry except for tail length, which indicated positive allometry
295 (slope of 1.437 (*maniculatus*) and 1.218 (*leucopus*), supplemental Figure 1).
296

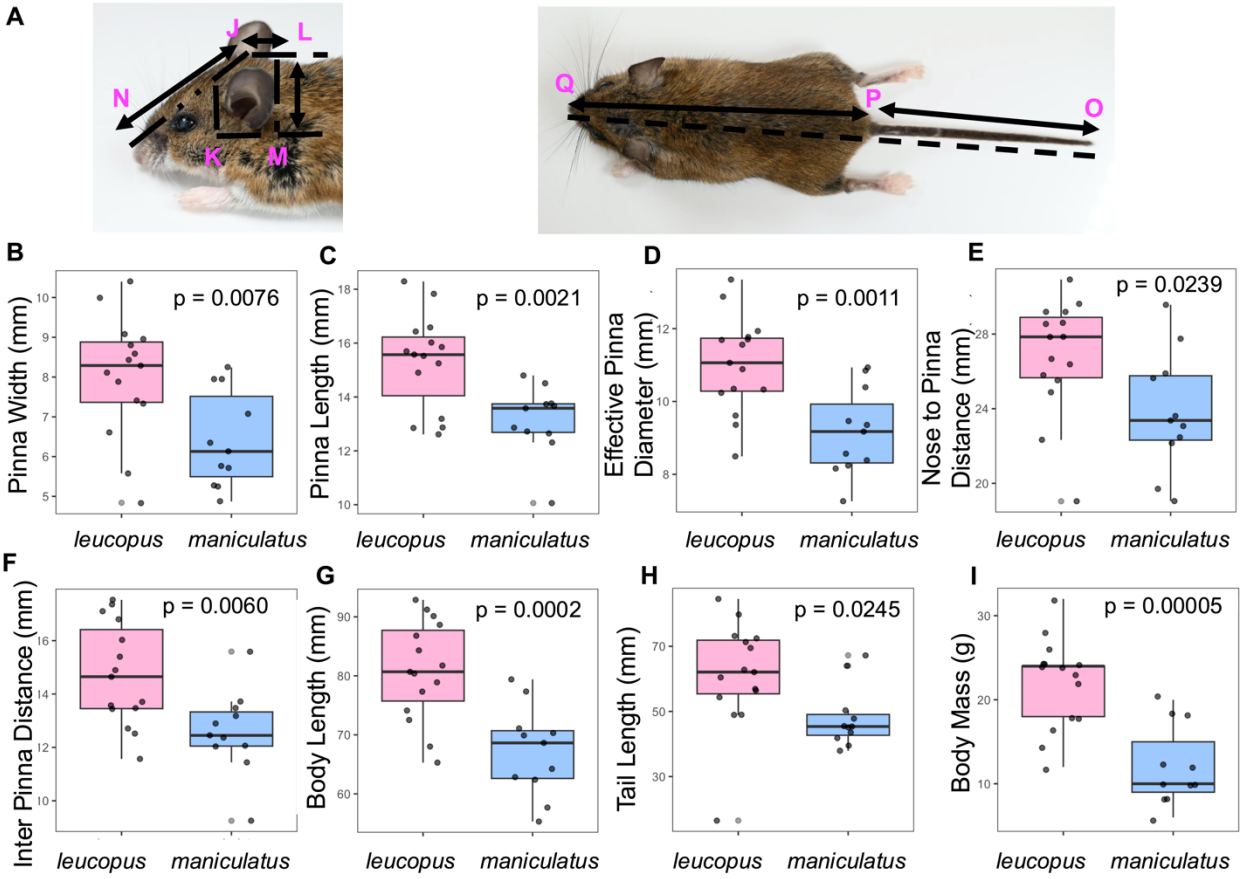

297

298 **Figure 3:** Morphological differences between *P. leucopus* and *P. maniculatus*. Pinnae, head, and body
299 features (**A**) were evaluated between species (pink boxplot = *leucopus*, blue boxplot = *maniculatus*).
300 Measurements JK show the inter pinnae distance, JN the nose to pinna distance, MK the pinna width, LM
301 the pinna height, OP the tail length, and PQ the body length. Effective pinna diameter was calculated by
302 taking the square root of pinna height multiplied by pinna width (MK/LM). Significant differences were
303 observed for all features including Pinna width (**B**), Pinna length (**C**), Effective diameter (**D**), Nose to
304 pinna distance (**E**), Inter pinna distance (**F**), Body length (**G**), Tail length (**H**), and Body mass (**I**).
305 Peromyscus pictured is a wild caught *P. leucopus* captured in Payne County, Stillwater, Oklahoma. Image
306 is presented only for demonstration of measurements.
307
308

Morphological characteristics	***Maniculatus* mean ± S. E**	***Leucopus* mean ± S. E**	**degrees of freedom**	**F-statistic**	**p-value**
Effective pinna diameter	9.16 ± 0.36	11.01 ± 0.34	1, 24	13.69	0.0011

Pinna length	13.15 ± 0.39	15.30 ± 0.45	1, 24	11.79	0.0021
Pinna width	6.42 ± 0.36	8.02 ± 0.39	1, 24	8.47	0.0076
Inter pinna distance	12.59 ± 0.47	14.72 ± 0.49	1, 24	9.08	0.0060
Nose to pinna distance	23.84 ± 0.96	26.82 ± 0.79	1, 24	5.82	0.0239
Body length	67.19 ± 2.28	80.87 ± 2.17	1, 24	18.32	0.0002
Tail length	48.01 ± 2.84	61.21 ± 4.21	1, 24	25.76	0.0245
Body mass	12 ± 1	22 ± 1	1, 24	24.2	0.00005

Table 2: Morphological characteristics features of *P. maniculatus* and *P. leucopus* of the Packsaddle wildlife management area (WMA), James Collin wildlife management area (WMA) and Payne County. Values presented represent the mean of different morphological features recorded ± standard error, the degrees of freedom, F-statistic, and p-value of morphological differences between species.

Frequency thresholds between species

Both *P. maniculatus* and *P. leucopus* displayed the best sensitivity to tones between 8 to 24 kHz, as indicated by lower ABR thresholds (Figure 4C). We detected no significant statistical difference in best frequency thresholds between species across the frequencies tested (LMM, $p = 0.4692$). Similarly, no significant difference in best frequency hearing threshold was observed between male and female *P. leucopus* ($F = 0.054$, $p = 0.82$). We next investigated whether craniofacial or pinna measurements features are correlated with or influence best frequency thresholds in both species. We found that none of the morphological measurements had a significant effect on best frequency hearing threshold between species (p-value > 0.05) (supplemental materials, Figure 3).

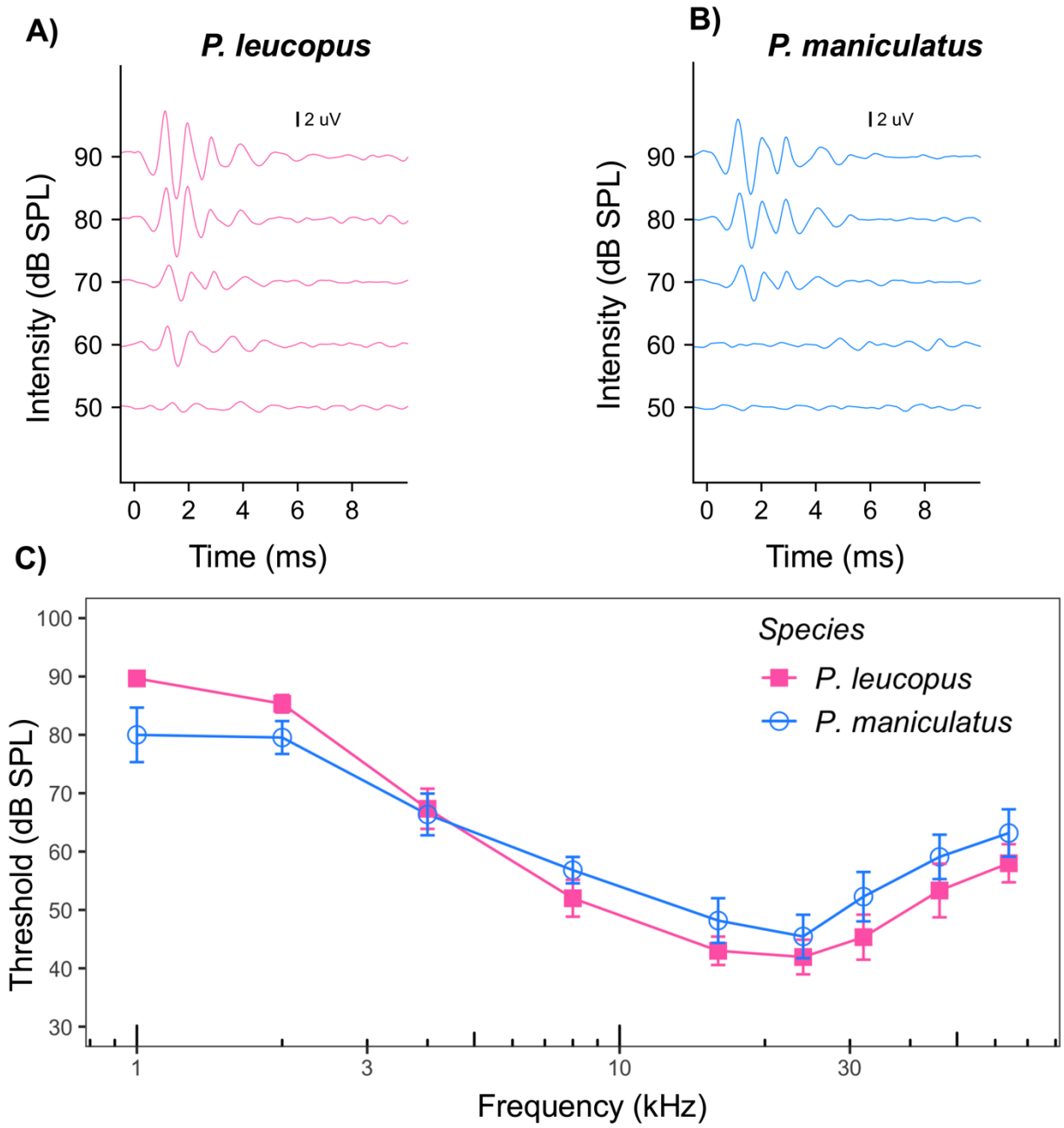

Figure 4: Figure 4A and 4B show Auditory Brainstem response patterns of a female *P. leucopus* and a female *P. maniculatus* determined with clicks of different intensities, respectively. Hearing range was measured across frequency (1-64 kHz) for both *P. leucopus* and *P. maniculatus* (Figure 4C). No significant main effects of frequency between species were found. Unfilled blue circles represent *P. maniculatus* while filled pink squares represent *P. leucopus*.

336 **ABR waveform amplitudes**

337 We measured the responses of *P. leucopus* and *P. maniculatus* to monaural transient
338 click stimuli across intensities (60 -90 dB SPL) to ensure responses above threshold. We
339 observed that the amplitude of waves I and IV (Figure 5A and 5B, wave I filled circles and wave
340 IV unfilled circles), increased monotonically with increasing intensity (60 to 90 dB SPL). At 90
341 dB SPL, the average amplitude of wave I and wave IV were 2.75 and 1.79 μV for *P. leucopus*.
342 For *P. maniculatus*, the average amplitude of wave I and wave IV were 3.27 and 1.83 μV at 90
343 dB SPL. *P. leucopus* monaural wave I and IV amplitude were statistically different across
344 intensities (LMM: p-value < 0.0001). There were no significant statistical differences in
345 monaural wave I and IV amplitude between male and female *P. leucopus* across intensities
346 (LMM: p-value = 0.677). Similarly, we detected significant main effects of intensity on
347 monaural wave I and IV amplitude of *P. maniculatus* (LMM: p-value = 0.002). For both species,
348 wave IV generally had smaller amplitude than wave I (Figure 5A and 5B: unfilled vs filled
349 circles) and as a result, the wave IV/I amplitude ratio was generally lower than 1.0 at most
350 intensities tested in both species (Figure 5A, 5B: diamond with dotted line).
351
352 **Monaural Amplitude Ratio**

353 Monaural amplitude ratio was calculated by dividing the amplitude value of wave IV by
354 the amplitude value of wave I for left and right pinnae at each intensity. As displayed in figure
355 5C, the wave IV/I amplitude ratio typically decreased with increasing intensity from 60 to 90 dB
356 SPL for both species (Figure 5A, 5B). A linear mix-effect model revealed significant statistical
357 differences of intensity on the amplitude ratio for *P. maniculatus* (LMM: p-value = 0.014).
358 However, no statistically significant differences of either intensity or sexes were observed on the

359 amplitude ratio for *P. leucopus* (Intensity: LMM: p-value = 0.332; Sex: LMM: p-value = 0.84).
360 When combined, the results of the linear mix-effect model revealed no significant main effects
361 of either intensity (LMM: p-value = 0.332) or species (LMM: p-value = 0.474) on the amplitude
362 ratio of wave I and IV between species.
363

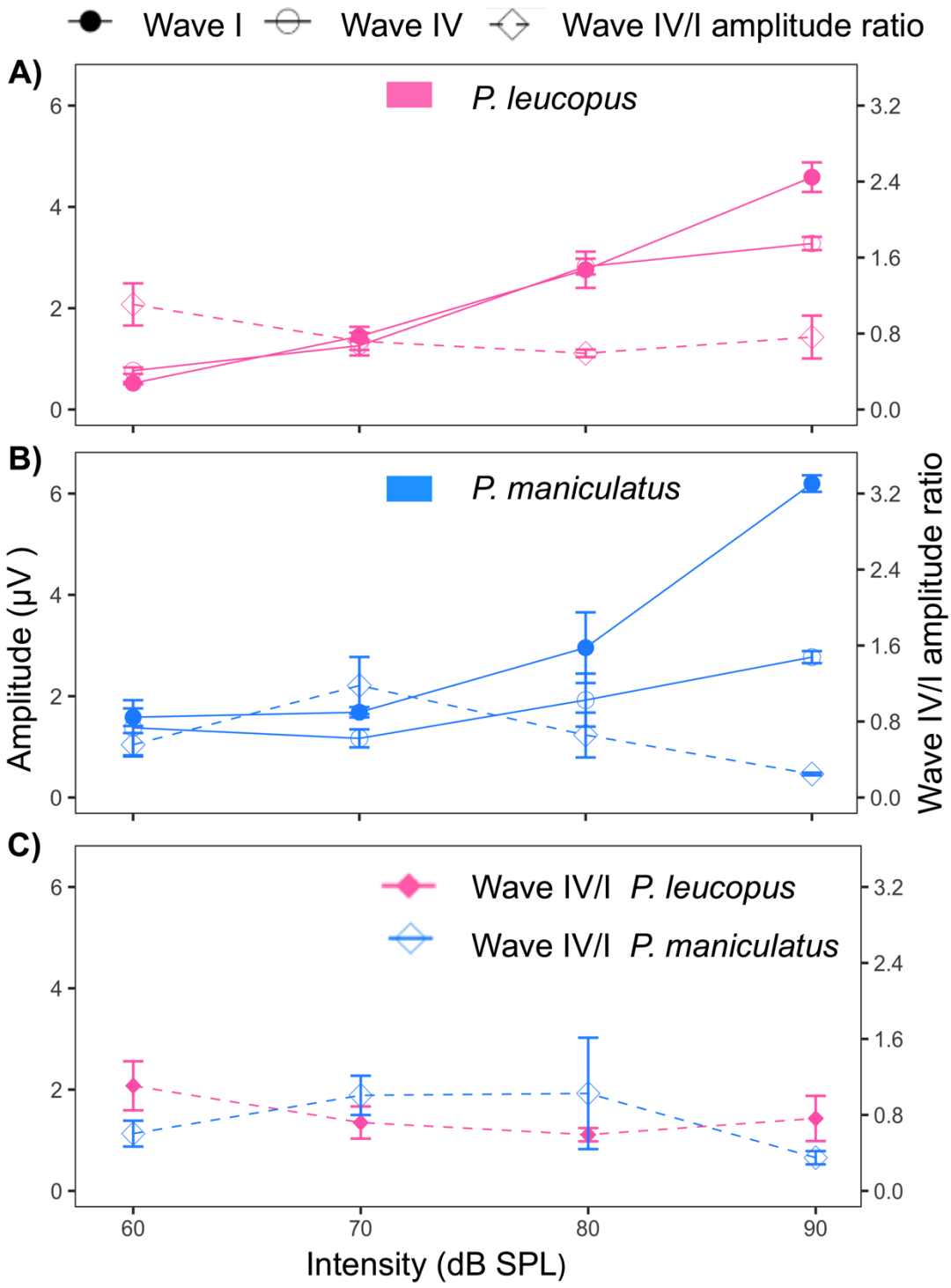

Figure 5: Average amplitude of wave I (filled circles) and wave IV (unfilled circles) of auditory brainstem responses determines with clicks of different intensities (Pink = *P. leucopus* (n = 15), Blue = *P. maniculatus* (n = 11)). The average wave IV/I amplitude ratio at each intensity (filled diamond with dotted line represents wave IV/I for *P. leucopus* and unfilled diamond with dotted line represents wave IV/I for *P. maniculatus*) is shown in each figure (right ordinate). The vertical bars represent the standard error at each point. Significant main effects of intensity on wave I and IV amplitude were detected for each species.

371
372 **Absolute Latency**

373 We next calculated the average peak latency of waves I and IV of both studied species
374 across click intensities (60 to 90 dB SPL). We detected no significant decrease in peak latency
375 for either wave I or wave IV with increasing intensity for *P. leucopus* (Wave I: LMM: p-value =
376 0.353; Wave IV: LMM: p-value = 0.122) (Figure 6A). Similarly, no significant statistical
377 differences were observed in peak latency for either wave I and wave IV between male and
378 female *P. leucopus* (Wave I: LMM: p-value = 0.841; Wave IV: p-value = 0.341). There were no
379 significant statistical differences in peak latency for either wave I or wave IV with increasing
380 intensity for *P. maniculatus* (Wave I: LMM: p-value = 0.353; wave IV: LMM: p-value = 0.392)
381 (Figure 6B). When data were combined, we detected no significant main effects of either
382 intensity or species in peak latency for either wave I or wave IV with increasing intensity
383 between both species (LMM: All p-value >0.05).

384

385 **Inter-peak latency**

386 Inter-peak latency was calculated as the difference in latency from the wave I peak to
387 the other designated peak (IV) for left and right pinnae at each intensity. We observed a
388 significant decreased in wave I-IV inter peak latency (Figure 6C) with increasing intensity for *P.*
389 *leucopus* (LMM: p-value = 0.043). However, no significant decrease in wave I-IV inter peak
390 latency was detected with increasing intensity between male and female *P. leucopus* (LMM: p-
391 value = 0.341). There was a significant decrease in wave I-IV inter peak latency (Figure 6C) with
392 increasing intensity for *P. maniculatus* (LMM: p-value = 0.010). When data were combined, we
393 observed a significant main effect of intensity on the inter-peak latency of waves I and IV

394 between both species (LMM: p-value = 0.002). However, no main effect of species was detected
395 on the inter-peak latency of waves I and IV between both species (LMM: p-value = 0.145).
396

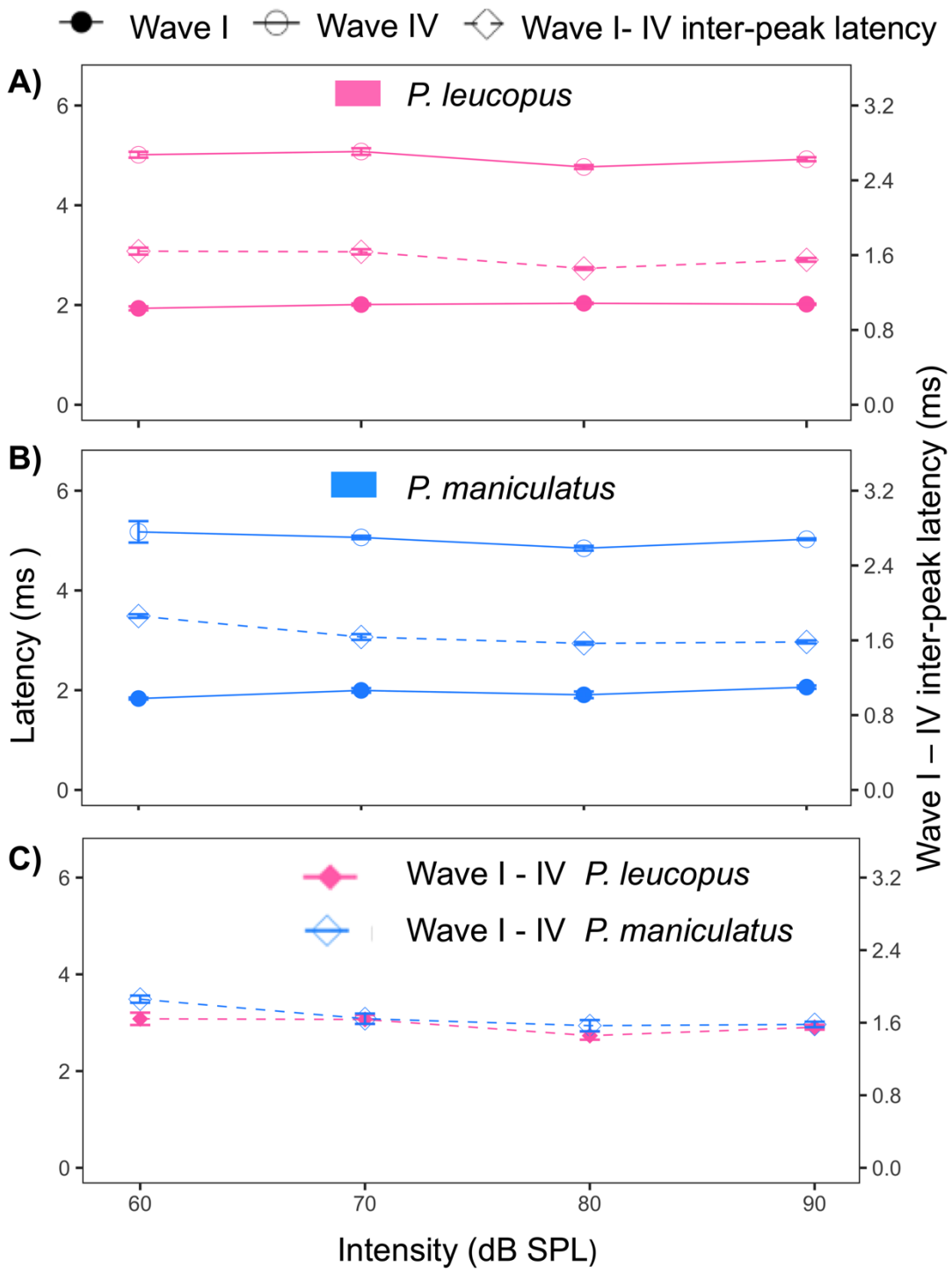

397

Figure 6: Average peak latency of wave I (filled circles) and wave IV (unfilled circles) of auditory brainstem responses determined with clicks of different intensities (Pink = *P. leucopus* (n = 15), Blue = *P. maniculatus* (n = 11)). The average wave I-IV inter-peak latency at each intensity (filled diamond with dotted line represents wave I-IV for *P. leucopus* and unfilled diamond with dotted line represents wave I-IV for *P. maniculatus*) is shown in each figure (right ordinate). The vertical bars represent the standard error at each point.

Slope latency intensity function between species

Peak latency is the time interval between the presentation of a sound stimulus and the peak at maximum amplitude of the designated wave. For both waves I and IV, we calculated the slope of each latency intensity function following the methods outlined by Zhou et al. 2006 (Figure 2 B(a), B(b), View methods section). As displayed in figure 3B, the slope of latency-intensity function of the exemplar female *P. leucopus* rodent was 7.80 µs/dB for wave I and 11.33 µs/dB for wave IV. *P. leucopus* had an average slope latency-intensity function of 6.386 µs/dB for wave I and 14.088 µs/dB for wave IV, while the average slope of latency-intensity function for wave I and wave IV of *P. maniculatus* was 7.291 µs/dB and 12.905 µs/dB, respectively (Figure 7). We detected significant main effects of wave number on slope of the latency-intensity function (LMM: p-value = 0.0003). However, no significant main effects of species were detected on slope of the latency-intensity function of both waves I and IV (LMM: p-value = 0.906). No pairwise comparisons were made for species since there was no main effect. A linear mix-effect model revealed that the slope of the latency-intensity function of wave IV was larger than wave I in both *P. leucopus* (t-value = -3.562, p-value = 0.001), and *P. maniculatus* (t-value = -2.084, p-value = 0.048).

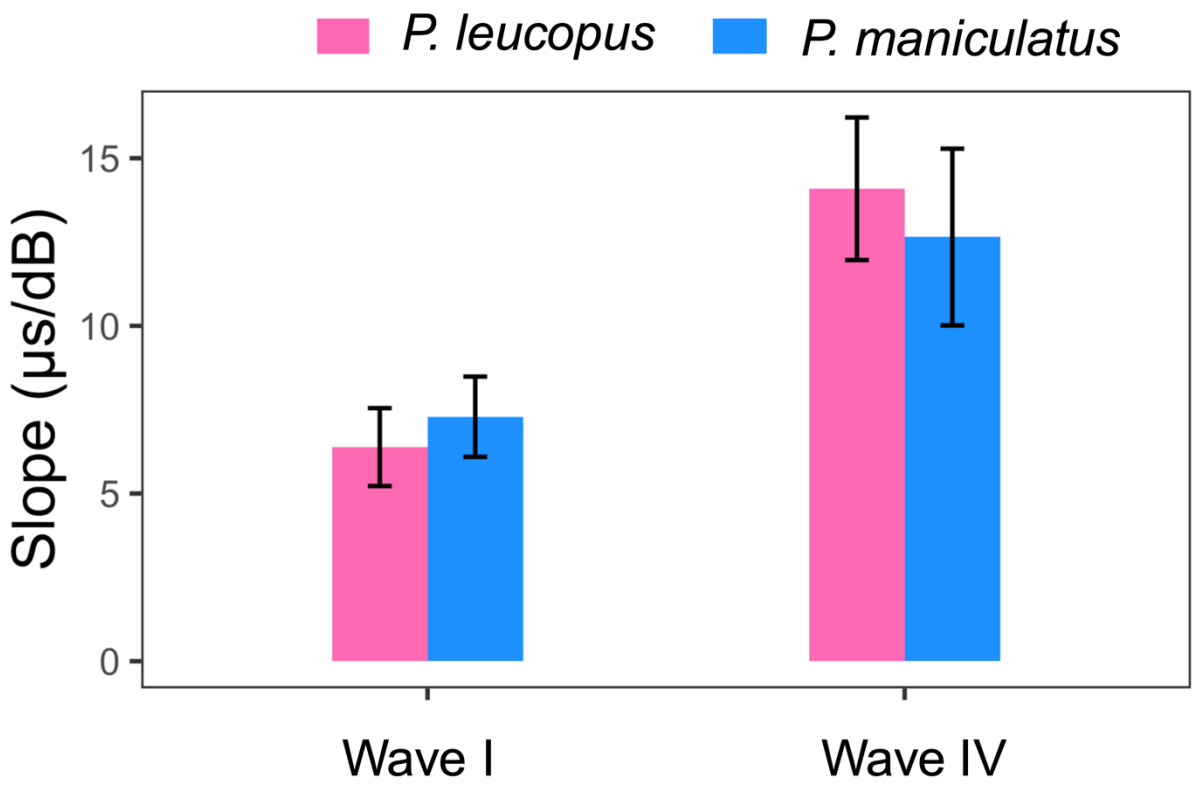

Figure 7: Average slope of latency-intensity function of waves I, and IV of ABRs (Pink = *P. leucopus* (n = 15), Blue = *P. maniculatus* (n = 11)).

Binaural hearing measures

We used the latency shift of the DN1 component of the BIC and relative DN1 amplitude to show the relationship of ITD on the latency and relative amplitude of the BIC in both studied species. The average DN1 amplitudes at 0 ITD were 2.72 µV and 1.74 µV for *P. maniculatus* and *P. leucopus*, respectively. The average latency for the DN1 component for 0 ITD was 5.01 ms for *P. maniculatus*, compared with 5.6 ms for *P. leucopus*. Linear mixed-effects models indicated no significant differences between *P. maniculatus* and *P. leucopus* across relative DN1 amplitude in relation to ITD normalized to the DN1 amplitude for 0 ITD (Figure 8B) (LMM: p-value = 0.82). Similarly, there were no significant statistical differences across relative amplitude in relation to ITD normalized to the DN1 amplitude for 0 ITD between male and female *P.*

437 *leucopus* (LMM: p-value > 0.05). There were statistically significant differences in latency shift
438 of the DN1 component of the BIC in relation to ITD normalized for 0 ITD between *P.*
439 *maniculatus* and *P. leucopus* (Figure 8A) (LMM: p = 0.016). Shift in DN1 latencies of the BIC
440 were significantly faster in *P. maniculatus* compared to *P. leucopus* at 1.0 ms (t-value = 2.101, p-
441 value = 0.037) and 2.0 ms (t-value = 2.316, p-value = 0.022) ITD (Figure 8A). When we added
442 body size to our LMM to test if body size contributes to BIC latencies, we saw a significant
443 effect of body size with a significant effect of species (all p-values < 0.05). We detected no
444 significant statistical differences in latency shift of the DN1 component of the BIC in relation to
445 ITD normalized for 0 ITD between male and female *P. leucopus* (LMM: p-value = 0.843).

446
447

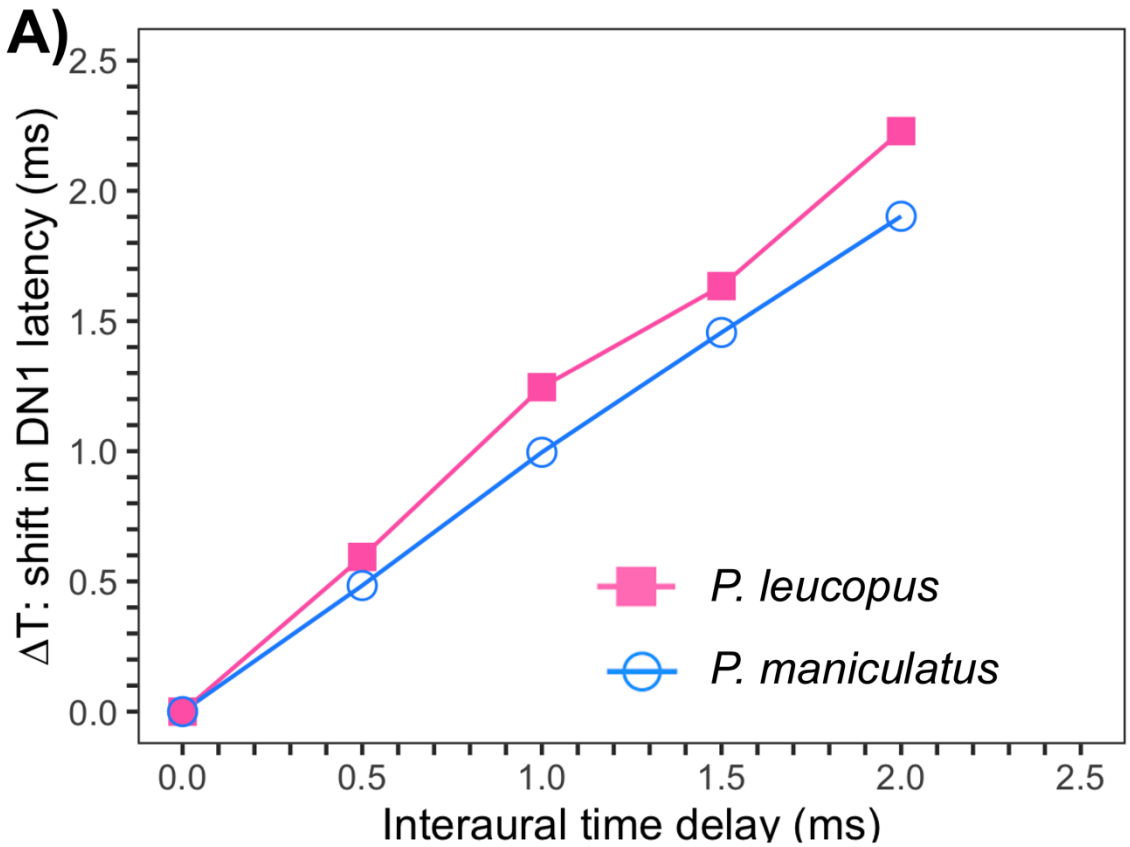

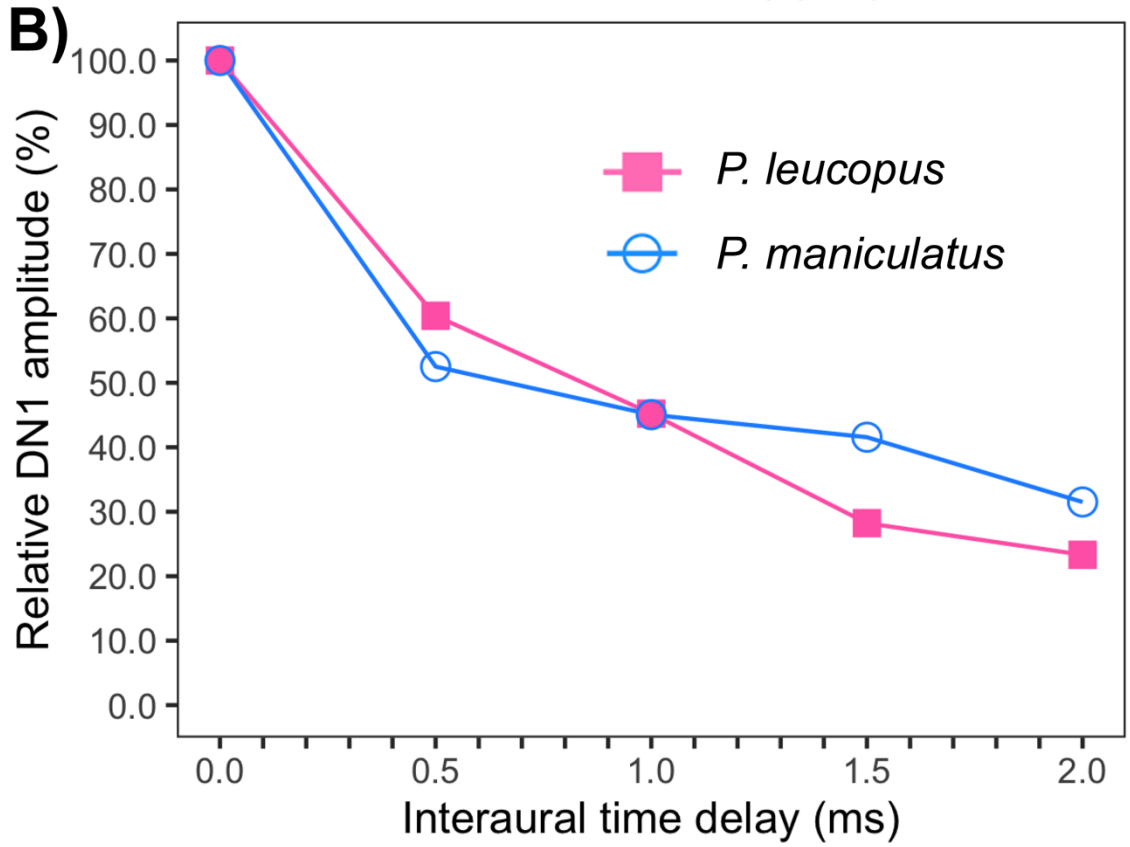

448

Figure 8: Binaural ABRs in wild *P. leucopus* (pink filled square) and *P. maniculatus* (blue unfilled circle). 8A, Shift in DN1 latency (ms) relative to ITD; reference latency at ITD = 0 is set to 0 ms. 8B, percentage relative DN1 amplitude relative to ITD normalized to the DN1 amplitude for ITD = 0 ms. Relative amplitude and latency of the DN1 BIC with varying ITD between - 2 to + 2 ms in 0.5 ms steps were measured. Significant differences were detected in BIC shift in DN1 latencies between both species at ITDs 1.0 and 2.0 ms. No significant differences were observed between both species for relative amplitude of the BIC across ITDs.

DISCUSSION

In this study, we used craniofacial morphology, pinna features, and ABRs to compare morphological features important for hearing with physiological measures of ABR amplitude and latency of two species of the genus *Peromyscus*. Like previous findings (Choate, 1973; Light et al., 2021; Millien et al., 2017), we detected significant morphological differences between both species including pinna length, pinna width, effective pinna diameter, inter-pinna distance, and other measures with *P. leucopus* displaying larger features. ABR-derived detection threshold revealed that both species share similar ABR response threshold across frequencies with the best frequency hearing between 8-24 kHz, which is in agreement with previous findings that showed *Peromyscus* species have best hearing sensitivity between 8-16 kHz (Capshaw et al., 2022; Dice and Barto, 1952; Ralls, 1967). Significant main effects of intensity were detected in monaural amplitude of ABR wave I and IV between both studied species, which is in accordance with similar findings using laboratory strains mice (Zhou et al., 2006). Measurements of the BIC, indicated similar amplitude across ITDs with differences in latency of the BIC across ITDs between the two species. Overall, our results revealed that both species have similar ABR best frequency threshold with *P. maniculatus* slightly having shorter latency BIC and smaller anatomical features compared to *P. leucopus*.

476 Morphological features including cranial size and shape, size of the pinnae, body and tail
477 length differ widely within species of the genus *Peromyscus* (Light et al., 2021; Ordóñez-Garza
478 et al., 2010). Our data showed differences in all measured anatomical traits between species
479 consistent with previous studies (Choate, 1973; Light et al., 2021; Millien et al., 2017). Previous
480 studies used two-dimensional (2D) geometric morphometrics (Light et al., 2021), and micro-CT
481 (Riede et al., 2022) as tools to morphologically differentiate rodents of the genus *Peromyscus*.
482 Light *et al* (2021) showed differences between *P. leucopus* and *P. maniculatus* based on head
483 size, pinnae features, hindfoot length, and other morphological features. Consistency in
484 morphological features (pinna length, pinna width, and body weight) documented in this study
485 provide additional evidence supporting the use of these morphology traits as reliable indicators
486 for distinguishing species within the genus *Peromyscus*.
487
488 Using ABRs, Capshaw *et al.* (2022) observed decreased hearing sensitivity to frequencies
489 below 2 kHz in two laboratory *Peromyscus* species (*P. leucopus* and *P. californicus*). Our
490 findings are consistent with Capshaw *et al.* (2022), with hearing thresholds around 85 dB SPL at
491 frequencies below 2 kHz in both studied species, suggesting relatively poor hearing sensitivity of
492 both studied species to frequencies 1-2 kHz. Small-headed mammals generally are not as
493 sensitive to low frequencies and therefore do not generate significant directional information
494 using low frequencies, where differences in timing and intensity between pinnae are minimal
495 (Lauer et al., 2018). Therefore, it is thought that small mammals rely on high frequencies for
496 directional hearing with exception of some subterranean mammals including the naked mole-rat
497 (*Heterocephalus glaber*), the plain pocket gopher (*Geomys bursarius*), and the blind mole rat
498 (*Spalax ehrenbergi*) that lack the capability to localize sound and lack high frequency hearing

499 (Heffner and Heffner, 1993, 1992, 1990), though see (Barker et al., 2021; Gessele et al., 2016;
500 McCullagh et al., 2022). The limited ability of small mammals (with exception of Mongolian
501 gerbils, chipmunks, groundhogs, hamsters, and others), like members of the genus *Peromyscus*,
502 to detect low frequency sounds has been attributed to selective pressure linked with the absence
503 of cues for localizing sounds in the horizontal plane (Heffner et al., 2001). Therefore, it is not
504 surprising that we did not observe low frequency sensitivity between the two studied species in
505 this current investigation.
506
507 *P. leucopus* and *P. maniculatus* are both highly territorial and produce both sonic and
508 ultrasonic vocalizations between 0.8 to 28 kHz (sustained vocalizations: frequency ranges
509 between 10-25 kHz, sweep vocalization: frequencies above 25 kHz, and barks: frequency ranges
510 between 0.8 and 6 kHz) (Miller and Engstrom, 2012; Pomerantz and Clemens, 1981; Riede et al.,
511 2022). The frequency ranges of ultrasonic vocalizations of both studied species correlate with
512 their best frequency threshold (Figure 4C, best frequency threshold ranging from 8-24 kHz).
513 Related species' (California mouse, *P. californicus*) defensive and distress vocalizations are
514 known to be associated with sounds ranging from 2 -30 kHz (Rieger and Marler, 2018). While
515 limited studies have described distress and defensive vocalizations across the genus *Peromyscus*,
516 previous investigations have reported that members of this genus produce agonistic calls such as
517 chits and barks at frequencies between 6 to 15 kHz (Houseknecht, 1968; Pasch et al., 2017).
518 These agonistic calls are likely associated with lower auditory thresholds at these frequencies for
519 the genus *Peromyscus*. These findings suggest that the good match of *Peromyscus's* vocalization
520 with their frequency threshold sensitivity (8 – 24 kHz) likely contributes to vocal air-borne
521 communication in the wild. In addition, *Peromyscus* species are relatively long-lived but due to

limited studies on the ability of *Peromyscus* to hear sound, it is hard to speculate the physiological mechanisms that govern hearing sensitivity over their lifespan. It is possible that the decreased emission of mitochondrial reactive oxygen species and improved activity of antioxidant enzymes might play key roles in sustaining healthy auditory sensitivity across *Peromyscus* species (Csiszar et al., 2007).

The white-footed mice (*P. leucopus*) and the deer mice (*P. maniculatus*) occur throughout Oklahoma but generally occupy different habitats, with *P. maniculatus* being more common in grasslands and *P. leucopus* primarily inhabiting shaded forests (Hackney and Stancampiano, 2015; Stancampiano and Schnell, 2004). In our study, *P. leucopus* subjects were mainly captured in shrubland and forested habitats, while *P. maniculatus* subjects were found in open grassland habitats. Our findings revealed that *P. leucopus* has similar sensitivity to sound as *P. maniculatus* across all frequencies tested, except at 1 kHz (t-value = 2.009, p-value = 0.046), where *P. maniculatus* show slightly better hearing. One possibility is that slightly higher frequency hearing sensitivity of *P. leucopus* may have coevolved with their vocal signal characteristics to facilitate effective communication in forested and shrubland environments, where acoustic information is often encoded at higher frequencies (Charlton et al., 2019). In addition, weight distribution suggests that eight of the 11 *P. maniculatus* subjects in the current study were juveniles, while 10 of the 15 *P. leucopus* were adults. Age differences could also explain the shifted high frequency hearing in *P. leucopus* compared to *P. maniculatus,* as small shifts in audiogram threshold has been observed in *P. leucopus* with aging (Capshaw et al., 2022). A comparative study evaluating the vocalization content and sound attenuation of both species in their respective habitats, across different age groups, would shed novel insights into

how habitat-related factors and age might influence the evolution of sound reception and communication strategy both within and among closely related *Peromyscus* species.

Amplitude of wave I and IV tend to increase monotonically in most small mammals with increasing intensity when measured by click stimuli (Zhou et al., 2006). Similar patterns have been reported in other taxa commonly used in evoked potential studies (Backoff and Caspary, 1994; Neil J. Ingham, 1998). Observed differences in wave amplitudes between the two species is likely a result of difference in craniofacial size relative to body mass. Previous studies indicate that smaller craniofacial size with small body mass may bring the recording electrodes into closer proximity to the generators, resulting in larger amplitudes compared to those with large body mass (Merzenich et al. 1983). Prior publications indicate that other factors such as neural synchronicity and the number of neural elements firing in the generators can also contribute to the amplitude of ABR waves (Merzenich et al., 1983).

ABR wave amplitude can be affected by several factors including electrode position, animal body temperature, external noise, recording protocol, and equipment characteristics, therefore normalization between waves can help control for this variability. In humans, it has been shown that auditory deficits related to retrocochlear pathology may lead to a decrease in wave IV amplitude, and ultimately cause a decrease in the wave IV/I amplitude ratio (Arnold 2000). Our data revealed that the wave IV has a smaller amplitude than wave I in both species at most intensities tested, resulting in a wave IV/I smaller than 1.0 (Figure 5C). Previous work measuring ABR in inbred mouse strains, rats, gerbils, cats, guinea pigs, and humans indicated that the ABR waves I and II are generally larger amplitude than ABR waves III and IV, which is

568 in agreement to this current results (Moore, 1983). However, wave II and III are relatively larger
569 in rats and guinea pigs, while shifted to wave IV in cats and wave IV-V complex in humans
570 (Merzenich et al., 1983). Accordingly, the species-specific differences in individual ABR wave
571 amplitude may result from complex factors including the evolution of the central nervous
572 system, neuronal response characteristics within the brainstem, and the neural conduction
573 velocity.
574
575 The slope of the latency-intensity function when combined with ABR threshold has been
576 shown to be a useful parameter to estimate hearing sensitivity (Zhou et al., 2006). Previous
577 studies have reported the slope of the latency-intensity function of wave I and IV of different
578 laboratory inbred strains of mice, gerbils, cats, and humans (Burkard et al., 1990; Burkard and
579 Voigt, 1989; Fullerton et al., 1987; Zhou et al., 2006). Zhou et al. described that the slope of the
580 latency-intensity functions of wave I and IV were 4.1 to 14.0 μs/dB in laboratory inbred stains of
581 mice (BALB/cJ, C3H/HeJ/ SJL/J, CBA/j, ect.) (Zhou et al., 2006). In gerbils and rats, wave I and
582 IV slope latency-intensity function have been reported to be ~ 8 to 9 and ~13 to 16 μs/dB,
583 respectively (Burkard et al., 1990; Burkard and Voigt, 1989). Other publications reported that the
584 slope of the latency-intensity function of wave I and IV were ~14 to 16 μs/dB in cats (Fullerton
585 et al., 1987). In addition, the slope of the latency-intensity function of wave V and other ABR
586 waves was ~ 40 μs/dB in humans and Dalmatian puppies but were ~ 28 μs/dB in Beagle puppies
587 (Burkard and Hecox, 1983; Poncelet et al., 2000). Accordingly, we conclude that the slope of the
588 latency-intensity function of wild *Peromyscus* rodents ABR waves is similar to that of laboratory
589 inbred strain of mice and gerbils, slightly less than those of rats and cats, but significantly less
590 than those of humans and dogs.

591

592 ITD and ILD are two cues that animals with external pinnae use for sound localization.
593 ITDs are generally processed by neurons in the medial superior olive (MSO <2kHz) while ILDs
594 are mainly processed by neurons in the lateral superior olive (LSO >2 kHz) (Grothe et al., 2010;
595 Suzuki and Horiuchi, 1981). Previous studies reported that the mean DN1 amplitude at 0 ITD
596 was 0.2 μV in humans, about 5 μV in guinea pig, 1.8 μV in gerbil, and 2.3 μV in cats (Goksoy et
597 al., 2005; Jones and Van der Poel, 1990; Laumen et al., 2016a; Riedel and Kollmeier, 2006;
598 Ungan et al., 1997). Comparatively, the DN1 amplitude of 0 ITD of wild *Peromyscus* species is
599 similar to that of gerbils and cats, higher than that of humans and significantly lower than that of
600 guinea pig. Differences in DN1 amplitude at 0 ITD observed could be a result of smaller distance
601 of the recorded electrodes to the subjects, as well as electrode configuration, or other procedural
602 differences.

603

604 Numerous publications have reported that latency of the DN1 component in humans
605 ranges from 5.6 to 6.8 ms, while those of other animal models (gerbil, cats, guinea pig) range
606 from 3.7 to 4.8 ms (Goksoy et al., 2005; Jones and Van der Poel, 1990; Riedel and Kollmeier,
607 2006; Ungan et al., 1997). Our data of the latency DN1 component is consistent with latencies
608 observed in human and is somewhat slower than what is seen in other animal models. Our results
609 are similar with others that show the latency of the DN1 component increases with longer ITDs
610 in cats, gerbil, guinea pig, and humans (Goksoy et al., 2005; Laumen et al., 2016b; Riedel and
611 Kollmeier, 2006; Ungan et al., 1997). Indeed, it has been suggested that the increase in DN1
612 latency with increasing ITD reflects the anatomy and interaction between excitatory and
613 inhibitory neurons in the superior olivary complex (Karino et al., 2011).

We observed faster latencies in DN1 in *P. maniculatus* compared to *P. leucopus*. It is hard to speculate whether the difference in DN1 latency observed between both species is associated with head size or the number of cells in the SOC nuclei. Studies characterizing the number of excitatory and inhibitory cells in the SOC of both species would be beneficial to allow for evaluation of the effects of head size or MSO and LSO size in shifts of the DN1 latency among *Peromyscus* species. Further studies involving more *Peromyscus* species and other techniques, such as head-related transfer functions, are needed to assess if larger external pinna sizes contribute to additional features of *Peromyscus* hearing such as the use of spectral notches and the contribution of the pinna to horizontal cues like ITD and ILD, particularly since our in-ear presentation of ITD stimuli bypass the pinna. We calculated the functional interaural distance for each species by summing the mean inter-pinna distance and pinna width divided by the speed of sound in air to evaluate the availability of ITD cues for each species. While this technique is limited due to our use of calipers and is not exactly the same as the time delay caused by sound traveling around the head, we nonetheless used this is to roughly estimate the functional interaural distance for each species. We found that *P. maniculatus* have a shorter functional interaural distance (± 55 μs) compared to *P. leucopus* (± 67 μs) which is consistent with smaller heads in *P. maniculatus*.

There are some limitations to the techniques employed in this study. Calipers are less accurate as features get smaller due to their measurement sensitivity, therefore measures of pinna and head morphology are likely to be less accurate than larger measurements such as body length and tail length. We conducted analyses correcting for overall body length; however, they did not

637 show significant positive allometry (slope > 1) indicating that either these features were not
638 allometric or the loss of accuracy of measurements at smaller distances contributed significantly
639 to error. However, the one measurement that showed positive allometry was tail length, which is
640 one of the longer, or perhaps more accurate, measures suggesting that finer measurement tools
641 might be needed to make further arguments about effects of overall body size and morphological
642 features on hearing in these species. There are also limitations to using ABRs as measures of
643 hearing, including that interpretation of thresholds using visual observation, as performed in our
644 study, can be subjective (Suthakar and Liberman, 2019). However, others have shown minimal
645 differences between algorithms and observers to auditory threshold measurements (Capshaw et
646 al., 2022). Further validation of our observer method with more quantitative algorithms would be
647 useful to confirm threshold values reported here, though our thresholds coincide well with the
648 published literature in one of these species (Capshaw et al., 2022). Lastly, behavioral measures
649 of hearing can show differences compared to ABRs, and indeed anesthetics used, montage of
650 electrodes, calibration of sounds (in ear or other methods), sound presentation, and other factors
651 all may influence ABR results making cross-species and cross-publication results difficult to
652 interpret (Ramsier and Dominy, 2010; Wolski et al., 2003). However, the current study used the
653 same parameters across both species and showed results consistent with the literature and what
654 might be expected for species that are closely related but differ primarily in size giving us
655 confidence in the results presented here.
656
657 **CONCLUSIONS**
658 Our findings provide a deeper understanding of auditory similarities and differences
659 between two species of *Peromyscus* and validate that the highly abundant *Peromyscus* may serve

as a future model for auditory studies. Both species show differences in craniofacial and pinna features and exhibit best hearing thresholds at frequencies ranging from 8 to 24 kHz. *P. maniculatus* showed shorter relative latencies of the DN1 component of the BIC, while relative DN1 amplitude was not different between the species. Further physiological assessment exploring hearing between the sexes at different ages and across the lifespan are needed to further show whether there are differences in hearing in under these conditions. In addition, clarifying the role of the BIC between sexes across species of the genus *Peromyscus* is important to understand its relevance for sex differences.

ACKNOWLEDGMENTS

We would like to thank Game wardens, Benny Farrar and Marcus Thibodeau for housing and giving us opportunities to sample at James Collin and Packsaddle Wildlife Management Areas. Also, we would like to thank members of team wild rodent of the McCullagh lab which helped in trapping and performed ABRs. We would also like to thank Dr. Tim Lei and Benzheng Li for their creation of the ABR acquisition and analysis custom python software. Dr. Fabio Machado helped with interpreting analyses of allometry and body size measurements. NIH NICHD funding 1R15HD105231-01 and 3R15HD105231-01S1, NSF RaMP DEB 2216648, and Oklahoma State University College of Arts & Sciences (CAS) Research Program to EAM helped fund summer support, RA support for LJ and undergraduates involved in the project, and some materials (CAS research award). Support for VYF was provided by a Wentz and CAS AURCA program support, and EMN with Wentz fellowship support as well as additional support for LJ from the Payne County Audubon Society.

DATA AVAILABILITY

The data of the study will be made available upon request.

AUTHOR CONTRIBUTIONS

LJ, EMN, TCW, VYF, And DMJ captured the animals and LJ and EMN collected the ABR data for the manuscript. LJ, DMJ, and GOUW performed DNA analysis on tails snip samples while BL helped with data analysis and interpretation. LJ and EAM completed the statistical analysis and developed the idea of the paper. LJ wrote the manuscript and all other authors revised and edited the manuscript.

COMPETING INTERESTS

The authors declare no competing interests.

REFERENCES

Anbuhl, K.L., Benichoux, V., Greene, N.T., Brown, A.D., Tollin, D.J., 2017. Development of the head, pinnae, and acoustical cues to sound location in a precocial species, the guinea pig (Cavia porcellus). Hearing Research 356, 35–50. https://doi.org/10.1016/j.heares.2017.10.015

Arnold: The auditory brainstem response - Google Scholar, n.d.

Backoff, P.M., Caspary, D.M., 1994. Age-related changes in auditory brainstem responses in fischer 344 rats: effects of rate and intensity. Hearing Research 73, 163–172. https://doi.org/10.1016/0378-5955(94)90231-3

Barker, A.J., Koch, U., Lewin, G.R., Pyott, S.J., 2021. Hearing and Vocalizations in the Naked Mole-Rat, in: Buffenstein, R., Park, T.J., Holmes, M.M. (Eds.), The Extraordinary Biology of the Naked Mole-Rat. Springer International Publishing, Cham, pp. 157–195. https://doi.org/10.1007/978-3-030-65943-1_6

Bates, D., Mächler, M., Bolker, B., Walker, S., 2014. Fitting Linear Mixed-Effects Models using lme4. https://doi.org/10.48550/ARXIV.1406.5823

Bedford, N.L., Hoekstra, H.E., 2015. Peromyscus mice as a model for studying natural variation. eLife 4, e06813. https://doi.org/10.7554/eLife.06813

Benichoux, V., Ferber, A., Hunt, S., Hughes, E., Tollin, D., 2018. Across Species "Natural Ablation" Reveals the Brainstem Source of a Noninvasive Biomarker of Binaural Hearing. J. Neurosci. 38, 8563–8573. https://doi.org/10.1523/JNEUROSCI.1211-18.2018

Blauert, J., 1997. Spatial Hearing: The Psychophysics of Human Sound Localization. MIT Press.

Bradley, R.D., Durish, N.D., Rogers, D.S., Miller, J.R., Engstrom, M.D., Kilpatrick, C.W., 2007. Toward a Molecular Phylogeny for Peromyscus: Evidence from Mitochondrial Cytochrome-b Sequences. Journal of Mammalogy 88, 1146–1159. https://doi.org/10.1644/06-MAMM-A-342R.1

Brittan-Powell, E.F., Dooling, R.J., 2004. Development of auditory sensitivity in budgerigars (*Melopsittacus undulatus*). The Journal of the Acoustical Society of America 115, 3092–3102. https://doi.org/10.1121/1.1739479

Burger, J., Gochfeld, M., 1992. Survival and reproduction in Peromyscus leucopus in the laboratory: viable model for aging studies. Growth Dev Aging 56, 17–22.

Burkard, R., Feldman, M., Voigt, H.F., 1990. Brainstem Auditory-Evoked Response in the Rat Normative Studies, with Observations Concerning the Effects of Ossicular Disruption. Audiology 29, 146–162. https://doi.org/10.3109/00206099009072847

Burkard, R., Hecox, K., 1983. The effect of broadband noise on the human brainstem auditory evoked response. I. Rate and intensity effects. The Journal of the Acoustical Society of America 74, 1204–1213. https://doi.org/10.1121/1.390024

Burkard, R., Voigt, H.F., 1989. Stimulus dependencies of the gerbil brain-stem auditory-evoked response (BAER). I: Effects of click level, rate, and polarity. The Journal of the Acoustical Society of America 85, 2514–2525. https://doi.org/10.1121/1.397746

Caire, W., 1989. Mammals of Oklahoma. University of Oklahoma Press.

Capshaw, G., Brown, A.D., Peña, J.L., Carr, C.E., Christensen-Dalsgaard, J., Tollin, D.J., Womack, M.C., McCullagh, E.A., 2023. The continued importance of comparative

763 auditory research to modern scientific discovery. Hearing Research 433, 108766.
764 https://doi.org/10.1016/j.heares.2023.108766
765 Capshaw, G., Vicencio-Jimenez, S., Screven, L.A., Burke, K., Weinberg, M.M., Lauer, A.M.,
766 2022. Physiological Evidence for Delayed Age-related Hearing Loss in Two Long-lived
767 Rodent Species (Peromyscus leucopus and P. californicus). JARO 23, 617–631.
768 https://doi.org/10.1007/s10162-022-00860-4
769 Charlton, B.D., Owen, M.A., Swaisgood, R.R., 2019. Coevolution of vocal signal characteristics
770 and hearing sensitivity in forest mammals. Nat Commun 10, 2778.
771 https://doi.org/10.1038/s41467-019-10768-y
772 Chawla, A., McCullagh, E.A., 2022. Auditory Brain Stem Responses in the C57BL/6J Fragile X
773 Syndrome-Knockout Mouse Model. Frontiers in Integrative Neuroscience 15.
774 Childs, J.E., Ksiazek, T.G., Spiropoulou, C.F., Krebs, J.W., Morzunov, S., Maupin, G.O., Gage,
775 K.L., Rollin, P.E., Sarisky, J., Enscore, R.E., Frey, J.K., Peters, C.J., Nichol, S.T., 1994.
776 Serologic and Genetic Identification of Peromyscus maniculatus as the Primary Rodent
777 Reservoir for a New Hantavirus in the Southwestern United States. Journal of Infectious
778 Diseases 169, 1271–1280. https://doi.org/10.1093/infdis/169.6.1271
779 Choate, J.R., 1973. Identification and Recent Distribution of White-Footed Mice (Peromyscus)
780 in New England. Journal of Mammalogy 54, 41–49. https://doi.org/10.2307/1378871
781 Colburn, H.S., Zurek, P.M., Durlach, N.I., 1987. Binaural Directional Hearing—Impairments
782 and Aids, in: Yost, W.A., Gourevitch, G. (Eds.), Directional Hearing, Proceedings in Life
783 Sciences. Springer, New York, NY, pp. 261–278. https://doi.org/10.1007/978-1-4612-
784 4738-8_11
785 Csiszar, A., Labinskyy, N., Zhao, X., Hu, F., Serpillon, S., Huang, Z., Ballabh, P., Levy, R.J.,
786 Hintze, T.H., Wolin, M.S., Austad, S.N., Podlutsky, A., Ungvari, Z., 2007. Vascular
787 superoxide and hydrogen peroxide production and oxidative stress resistance in two
788 closely related rodent species with disparate longevity. Aging Cell 6, 783–797.
789 https://doi.org/10.1111/j.1474-9726.2007.00339.x
790 Cummings, J.R., Vessey, S.H., 1994. Agricultural Influences on Movement Patterns of White-
791 Footed Mice (Peromyscus leucopus). The American Midland Naturalist 132, 209–218.
792 https://doi.org/10.2307/2426575
793 Dammann, P., 2017. Slow aging in mammals—Lessons from African mole-rats and bats.
794 Seminars in Cell & Developmental Biology, Science communication in the field of
795 fundamental biomedical research 70, 154–163.
796 https://doi.org/10.1016/j.semcdb.2017.07.006
797 Dewey, M.J., Dawson, W.D., 2001. Deer mice: "The Drosophila of North American
798 mammalogy." genesis 29, 105–109. https://doi.org/10.1002/gene.1011
799 Dice, L.R., Barto, E., 1952. Ability of Mice of the Genus Peromyscus to Hear Ultrasonic Sounds.
800 Science 116, 110–111. https://doi.org/10.1126/science.116.3005.110
801 Ducroz, J.F., Volobouev, V., Granjon, L., 2001. An Assessment of the Systematics of
802 Arvicanthine Rodents Using Mitochondrial DNA Sequences: Evolutionary and
803 Biogeographical Implications. Journal of Mammalian Evolution 8, 173–206.
804 https://doi.org/10.1023/A:1012277012303
805 Ehret, G., Dreyer, A., 1984. Localization of tones and noise in the horizontal plane by
806 unrestrained house mice (Mus musculus). Journal of Experimental Biology 109, 163–
807 174. https://doi.org/10.1242/jeb.109.1.163

Fairbairn, D.J., 1977. The spring decline in deer mice: death or dispersal? Can. J. Zool. 55, 84–92. https://doi.org/10.1139/z77-009

Fiset, J., Tessier, N., Millien, V., Lapointe, F.-J., 2015. Phylogeographic Structure of the White-Footed Mouse and the Deer Mouse, Two Lyme Disease Reservoir Hosts in Québec. PLoS ONE 10, e0144112. https://doi.org/10.1371/journal.pone.0144112

Fullerton, B.C., Levine, R.A., Hosford-Dunn, H.L., Kiang, N.Y.S., 1987. Comparison of cat and human brain-stem auditory evoked potentials. Electroencephalography and Clinical Neurophysiology 66, 547–570. https://doi.org/10.1016/0013-4694(87)90102-7

Furst, M., Eyal, S., Korczyn, A.D., 1990. Prediction of binaural click lateralization by brainstem auditory evoked potentials. Hear Res 49, 347–359. https://doi.org/10.1016/0378-5955(90)90113-4

Gessele, N., Garcia-Pino, E., Omerbašić, D., Park, T.J., Koch, U., 2016. Structural Changes and Lack of HCN1 Channels in the Binaural Auditory Brainstem of the Naked Mole-Rat (Heterocephalus glaber). PLOS ONE 11, e0146428. https://doi.org/10.1371/journal.pone.0146428

Goksoy, C., Demirtas, S., Yagcioglu, S., Ungan, P., 2005. Interaural delay-dependent changes in the binaural interaction component of the guinea pig brainstem responses. Brain Research 1054, 183–191. https://doi.org/10.1016/j.brainres.2005.06.083

Grothe, B., Pecka, M., McAlpine, D., 2010. Mechanisms of sound localization in mammals. Physiol Rev 90, 983–1012. https://doi.org/10.1152/physrev.00026.2009

Guo, Z., Wang, M., Tian, G., Burger, J., Gochfeld, M., Yang, C.S., 1993. Age- and gender-related variations in the activities of drug-metabolizing and antioxidant enzymes in the white-footed mouse (Peromyscus leucopus). Growth Dev Aging 57, 85–100.

Hackney, S., Stancampiano, A.J., 2015. Microhabitat Preferences of a Small Mammal Assemblage in Canadian County, Oklahoma. Proceedings of the Oklahoma Academy of Science 95.

Harney, B.A., Dueser, R.D., 1987. Vertical Stratification of Activity of Two Peromyscus Species: An Experimental Analysis. Ecology 68, 1084–1091. https://doi.org/10.2307/1938380

Heeringa, A.N., Zhang, L., Ashida, G., Beutelmann, R., Steenken, F., Köppl, C., 2020. Temporal Coding of Single Auditory Nerve Fibers Is Not Degraded in Aging Gerbils. J. Neurosci. 40, 343–354. https://doi.org/10.1523/JNEUROSCI.2784-18.2019

Heffner, H.E., Heffner, R.S., 1985. Hearing in two cricetid rodents: Wood rat (Neotoma floridana) and grasshopper mouse (Onychomys leucogaster). Journal of Comparative Psychology 99, 275–288. https://doi.org/10.1037/0735-7036.99.3.275

Heffner, H.E.H., Rickye S., 2001. Behavioral Assessment of Hearing in Mice, in: Handbook of Mouse Auditory Research. CRC Press.

Heffner, R.S., Heffner, H.E., 1993. Degenerate hearing and sound localization in naked mole rats (*Heterocephalus glaber*), with an overview of central auditory structures. J of Comparative Neurology 331, 418–433. https://doi.org/10.1002/cne.903310311

Heffner, R.S., Heffner, H.E., 1992. Hearing and sound localization in blind mole rats (*Spalax ehrenbergi*). Hearing Research 62, 206–216. https://doi.org/10.1016/0378-5955(92)90188-S

Heffner, R.S., Heffner, H.E., 1990. Vestigial hearing in a fossorial mammal, the pocket gopher (*Geomys bursarius*). Hearing Research 46, 239–252. https://doi.org/10.1016/0378-5955(90)90005-A

Heffner, R.S., Heffner, H.E., 1982. Hearing in the elephant (Elephas maximus): absolute sensitivity, frequency discrimination, and sound localization. J Comp Physiol Psychol 96, 926–944.

Heffner, R.S., Koay, G., Heffner, H.E., 2020. Hearing and sound localization in Cottontail rabbits, Sylvilagus floridanus. J Comp Physiol A 206, 543–552. https://doi.org/10.1007/s00359-020-01424-8

Heffner, R.S., Koay, G., Heffner, H.E., 2001. Audiograms of five species of rodents: implications for the evolution of hearing and the perception of pitch. Hearing Research 157, 138–152. https://doi.org/10.1016/S0378-5955(01)00298-2

Houseknecht, C.R., 1968. Sonographic Analysis of Vocalizations of Three Species of Mice. Journal of Mammalogy 49, 555. https://doi.org/10.2307/1378232

Jones, S.J., Van der Poel, J.C., 1990. Binaural interaction in the brain-stem auditory evoked potential: evidence for a delay line coincidence detection mechanism. Electroencephalography and Clinical Neurophysiology/Evoked Potentials Section 77, 214–224. https://doi.org/10.1016/0168-5597(90)90040-K

Jüchter, C., Beutelmann, R., Klump, G.M., 2022. Speech sound discrimination by Mongolian gerbils. Hearing Research 418, 108472. https://doi.org/10.1016/j.heares.2022.108472

Karino, S., Smith, P.H., Yin, T.C.T., Joris, P.X., 2011. Axonal Branching Patterns as Sources of Delay in the Mammalian Auditory Brainstem: A Re-Examination. J. Neurosci. 31, 3016–3031. https://doi.org/10.1523/JNEUROSCI.5175-10.2011

Kidd, G., Mason, C.R., Rohtla, T.L., 1995. Binaural advantage for sound pattern identification. The Journal of the Acoustical Society of America 98, 1977–1986. https://doi.org/10.1121/1.414459

King, J.A., 1968. Biology of Peromyscus (Rodentia). Biology of Peromyscus (Rodentia).

Kirkland, G.L., Layne, J.N., 1989. Advances in the Study of Peromyscus (Rodentia) Texas Tech University Press. Lubbock, TX.

Labinskyy, N., Mukhopadhyay, P., Toth, J., Szalai, G., Veres, M., Losonczy, G., Pinto, J.T., Pacher, P., Ballabh, P., Podlutsky, A., Austad, S.N., Csiszar, A., Ungvari, Z., 2009. Longevity is associated with increased vascular resistance to high glucose-induced oxidative stress and inflammatory gene expression in Peromyscus leucopus. American Journal of Physiology-Heart and Circulatory Physiology 296, H946–H956. https://doi.org/10.1152/ajpheart.00693.2008

Larson, S.R., Lee, X., Paskewitz, S.M., 2018. Prevalence of Tick-Borne Pathogens in Two Species of Peromyscus Mice Common in Northern Wisconsin. Journal of Medical Entomology 55, 1002–1010. https://doi.org/10.1093/jme/tjy027

Lauer, A.M., Engel, J.H., Schrode, K., 2018. Rodent Sound Localization and Spatial Hearing, in: Dent, M.L., Fay, R.R., Popper, A.N. (Eds.), Rodent Bioacoustics, Springer Handbook of Auditory Research. Springer International Publishing, Cham, pp. 107–130. https://doi.org/10.1007/978-3-319-92495-3_5

Laumen, G., Ferber, A.T., Klump, G.M., Tollin, D.J., 2016a. The Physiological Basis and Clinical Use of the Binaural Interaction Component of the Auditory Brainstem Response. Ear Hear 37, e276–e290. https://doi.org/10.1097/AUD.0000000000000301

Laumen, G., Tollin, D.J., Beutelmann, R., Klump, G.M., 2016b. Aging effects on the binaural interaction component of the auditory brainstem response in the Mongolian gerbil: Effects of interaural time and level differences. Hearing Research 337, 46–58. https://doi.org/10.1016/j.heares.2016.04.009

Lewarch, C.L., Hoekstra, H.E., 2018. The evolution of nesting behaviour in Peromyscus mice. Animal Behaviour 139, 103–115. https://doi.org/10.1016/j.anbehav.2018.03.008

Light, J.E., Siciliano-Martina, L., Dohlanik, E.G., Hafner, D.J., Lawing, A.M., Greenbaum, I.F., Light, J.E., Siciliano-Martina, L., Dohlanik, E.G., Hafner, D.J., Lawing, A.M., Greenbaum, I.F., 2021. Morphological differentiation of Peromyscus leucopus and P. maniculatus in East Texas. Therya 12, 369–387. https://doi.org/10.12933/therya-21-1116

McCullagh, E.A., Peacock, J., Lucas, A., Poleg, S., Greene, N.T., Gaut, A., Lagestee, S., Zhang, Y., Kaczmarek, L.K., Park, T.J., Tollin, D.J., Klug, A., 2022. Auditory brainstem development of naked mole-rats (Heterocephalus glaber). Proceedings of the Royal Society B: Biological Sciences 289, 20220878. https://doi.org/10.1098/rspb.2022.0878

McCullagh, E.A., Poleg, S., Greene, N.T., Huntsman, M.M., Tollin, D.J., Klug, A., 2020. Characterization of Auditory and Binaural Spatial Hearing in a Fragile X Syndrome Mouse Model. eNeuro 7. https://doi.org/10.1523/ENEURO.0300-19.2019

Miller, J.R., Engstrom, M.D., 2012. Vocal stereotypy in the rodent genera Peromyscus and Onychomys (Neotominae): taxonomic signature and call design. Bioacoustics 21, 193–213. https://doi.org/10.1080/09524622.2012.675176

Millien, V., Ledevin, R., Boué, C., Gonzalez, A., 2017. Rapid morphological divergence in two closely related and co-occurring species over the last 50 years. Evol Ecol 31, 847–864. https://doi.org/10.1007/s10682-017-9917-0

Mills, J.H., Schmiedt, R.A., Kulish, L.F., 1990. Age-related changes in auditory potentials of mongolian gerbil. Hearing Research 46, 201–210. https://doi.org/10.1016/0378-5955(90)90002-7

Moore, E.J., 1983. Bases of auditory brain-stem evoked responses. Grune & Stratton.

Neil J. Ingham, S.K.T., Spiro D. Comis, Deborah J. Withington, 1998. The Auditory Brainstem Response of Aged Guinea Pigs. Acta Oto-Laryngologica 118, 673–680. https://doi.org/10.1080/00016489850183160

New, E.M., Hurd, J.A., Alarcon, G.A., Miller, C.S., Williams, P.A., Greene, N.T., Sergott, C.E., Li, B.-Z., Lei, T.C., McCullagh, E.A., 2024. Hearing ability of prairie voles (Microtus ochrogaster). J Acoust Soc Am 155, 555–567. https://doi.org/10.1121/10.0024357

Nicolas, V., Schaeffer, B., Missoup, A.D., Kennis, J., Colyn, M., Denys, C., Tatard, C., Cruaud, C., Laredo, C., 2012. Assessment of Three Mitochondrial Genes (16S, Cytb, CO1) for Identifying Species in the Praomyini Tribe (Rodentia: Muridae). PLOS ONE 7, e36586. https://doi.org/10.1371/journal.pone.0036586

Ohlemiller, K.K., Frisina, R.D., 2008. Age-Related Hearing Loss and Its Cellular and Molecular Bases, in: Schacht, J., Popper, A.N., Fay, R.R. (Eds.), Auditory Trauma, Protection, and Repair, Springer Handbook of Auditory Research. Springer US, Boston, MA, pp. 145–194. https://doi.org/10.1007/978-0-387-72561-1_6

Ordóñez-Garza, N., Matson, J.O., Strauss, R.E., Bradley, R.D., Salazar-Bravo, J., 2010. Patterns of phenotypic and genetic variation in three species of endemic Mesoamerican Peromyscus (Rodentia: Cricetidae). Journal of Mammalogy 91, 848–859. https://doi.org/10.1644/09-MAMM-A-167.1

Pasch, B., Tokuda, I.T., Riede, T., 2017. Grasshopper mice employ distinct vocal production mechanisms in different social contexts. Proc. R. Soc. B. 284, 20171158. https://doi.org/10.1098/rspb.2017.1158

Platt, R.N., II, Amman, B.R., Keith, M.S., Thompson, C.W., Bradley, R.D., 2015. What Is Peromyscus? Evidence from nuclear and mitochondrial DNA sequences suggests the

946 need for a new classification. Journal of Mammalogy 96, 708–719.
947 https://doi.org/10.1093/jmammal/gyv067
948 Pomerantz, S.M., Clemens, L.G., 1981. Ultrasonic vocalizations in male deer mice (Peromyscus
949 maniculatus bairdi): Their role in male sexual behavior. Physiology & Behavior 27, 869–
950 872. https://doi.org/10.1016/0031-9384(81)90055-X
951 Poncelet, L., Coppens, A., Deltenre, P., 2000. Brainstem Auditory Evoked Potential Wave V
952 Latency-Intensity Function in Normal Dalmatian and Beagle Puppies. Journal of
953 Veterinary Internal Medicine 14, 424–428. https://doi.org/10.1111/j.1939-
954 1676.2000.tb02251.x
955 Ralls, K., 1967. Auditory sensitivity in mice: Peromyscus and Mus musculus. Animal Behaviour
956 15, 123–128. https://doi.org/10.1016/S0003-3472(67)80022-8
957 Ramsier, M.A., Dominy, N.J., 2010. A comparison of auditory brainstem responses and
958 behavioral estimates of hearing sensitivity in Lemur catta and Nycticebus coucang.
959 American Journal of Primatology 72, 217–233. https://doi.org/10.1002/ajp.20780
960 Riede, T., Kobrina, A., Bone, L., Darwaiz, T., Pasch, B., 2022. Mechanisms of sound production
961 in deer mice (Peromyscus spp.). Journal of Experimental Biology 225, jeb243695.
962 https://doi.org/10.1242/jeb.243695
963 Riedel, H., Kollmeier, B., 2006. Interaural delay-dependent changes in the binaural difference
964 potential of the human auditory brain stem response. Hearing Research 218, 5–19.
965 https://doi.org/10.1016/j.heares.2006.03.018
966 Rieger, N.S., Marler, C.A., 2018. The function of ultrasonic vocalizations during territorial
967 defence by pair-bonded male and female California mice. Animal Behaviour 135, 97–
968 108. https://doi.org/10.1016/j.anbehav.2017.11.008
969 Robins, J.H., Hingston, M., Matisoo-Smith, E., Ross, H.A., 2007. Identifying *Rattus* species
970 using mitochondrial DNA. Molecular Ecology Notes 7, 717–729.
971 https://doi.org/10.1111/j.1471-8286.2007.01752.x
972 Russell, L., 2018. Emmeans: estimated marginal means, aka least-squares means. R package
973 version 1.
974 Sayers, E.W., Bolton, E.E., Brister, J.R., Canese, K., Chan, J., Comeau, D.C., Connor, R., Funk,
975 K., Kelly, C., Kim, S., Madej, T., Marchler-Bauer, A., Lanczycki, C., Lathrop, S., Lu, Z.,
976 Thibaud-Nissen, F., Murphy, T., Phan, L., Skripchenko, Y., Tse, T., Wang, J., Williams,
977 R., Trawick, B.W., Pruitt, K.D., Sherry, S.T., 2022. Database resources of the National
978 Center for Biotechnology Information. Nucleic Acids Research 50, D20.
979 https://doi.org/10.1093/nar/gkab1112
980 Sayers, E.W., Cavanaugh, M., Clark, K., Pruitt, K.D., Schoch, C.L., Sherry, S.T., Karsch-
981 Mizrachi, I., 2021. GenBank. Nucleic Acids Research 49, D92–D96.
982 https://doi.org/10.1093/nar/gkaa1023
983 Shi, Y., Pulliam, D.A., Liu, Y., Hamilton, R.T., Jernigan, A.L., Bhattacharya, A., Sloane, L.B.,
984 Qi, W., Chaudhuri, A., Buffenstein, R., Ungvari, Z., Austad, S.N., Van Remmen, H.,
985 2013. Reduced mitochondrial ROS, enhanced antioxidant defense, and distinct age-
986 related changes in oxidative damage in muscles of long-lived Peromyscus leucopus.
987 American Journal of Physiology-Regulatory, Integrative and Comparative Physiology
988 304, R343–R355. https://doi.org/10.1152/ajpregu.00139.2012
989 Sikes, R.S., Gannon, W.L., the Animal Care and Use Committee of the American Society of
990 Mammalogists, 2011. Guidelines of the American Society of Mammalogists for the use

of wild mammals in research. Journal of Mammalogy 92, 235–253. https://doi.org/10.1644/10-MAMM-F-355.1

Stancampiano, A.J., Schnell, G.D., 2004. Microhabitat Affinities of Small Mammals in Southwestern Oklahoma. Journal of Mammalogy 85, 948–958.

Suthakar, K., Liberman, M.C., 2019. A simple algorithm for objective threshold determination of auditory brainstem responses. Hearing Research 381, 107782. https://doi.org/10.1016/j.heares.2019.107782

Suzuki, T., Horiuchi, K., 1981. Rise Time of Pure-Tone Stimuli in Brain Stem Response Audiometry. Audiology 20, 101–112. https://doi.org/10.3109/00206098109072688

Ungan, P., Yağcioğlu, S., Özmen, B., 1997. Interaural delay-dependent changes in the binaural difference potential in cat auditory brainstem response: implications about the origin of the binaural interaction component 1. Hearing Research 106, 66–82. https://doi.org/10.1016/S0378-5955(97)00003-8

Voelkl, B., Altman, N.S., Forsman, A., Forstmeier, W., Gurevitch, J., Jaric, I., Karp, N.A., Kas, M.J., Schielzeth, H., Van de Casteele, T., Würbel, H., 2020. Reproducibility of animal research in light of biological variation. Nat Rev Neurosci 21, 384–393. https://doi.org/10.1038/s41583-020-0313-3

Vrana, P.B., Shorter, K.R., Szalai, G., Felder, M.R., Crossland, J.P., Veres, M., Allen, J.E., Wiley, C.D., Duselis, A.R., Dewey, M.J., Dawson, W.D., 2014. Peromyscus (deer mice) as developmental models. WIREs Developmental Biology 3, 211–230. https://doi.org/10.1002/wdev.132

Wang, Xin, Zhu, M., Samuel, O.W., Wang, Xiaochen, Zhang, H., Yao, J., Lu, Y., Wang, M., Mukhopadhyay, S.C., Wu, W., Chen, S., Li, G., 2020. The Effects of Random Stimulation Rate on Measurements of Auditory Brainstem Response. Frontiers in Human Neuroscience 14.

Wickham, H., 2016. Programming with ggplot2, in: Wickham, H. (Ed.), Ggplot2: Elegant Graphics for Data Analysis, Use R! Springer International Publishing, Cham, pp. 241–253. https://doi.org/10.1007/978-3-319-24277-4_12

Wolski, L.F., Anderson, R.C., Bowles, A.E., Yochem, P.K., 2003. Measuring hearing in the harbor seal (Phoca vitulina): Comparison of behavioral and auditory brainstem response techniques. The Journal of the Acoustical Society of America 113, 629–637. https://doi.org/10.1121/1.1527961

Zhou, X., Jen, P.H.-S., Seburn, K.L., Frankel, W.N., Zheng, Q.Y., 2006. Auditory brainstem responses in 10 inbred strains of mice. Brain Research 1091, 16–26. https://doi.org/10.1016/j.brainres.2006.01.107

Figure legends:

Figure 1: Map showing trapping site locations in Oklahoma. Packsaddle wildlife management area (WMA) sites are presented by yellow triangle, James Collin wildlife management area (WMA) sites are presented by blue squares, and Payne County sites are presented by red circle.

Figure 2: Auditory Brainstem response patterns of a female *P. leucopus* determined with clicks of different intensities. Peak latency of monaural wave I and IV decrease with increasing click intensity (dotted lines). B (a) represents latency intensity functions of wave I and B (b) shows

latency intensity functions of wave IV. The slope of the latency intensity function was calculated as the amount of change in peak latency per decibel.

Figure 3: Morphological differences between *P. leucopus* and *P. maniculatus*. Pinnae, head, and body features (**A**) were evaluated between species (pink boxplot = *leucopus*, blue boxplot = *maniculatus*). Measurements JK show the inter pinnae distance, JN the nose to pinna distance, MK the pinna width, LM the pinna height, OP the tail length, and PQ the body length. Effective pinna diameter was calculated by taking the square root of pinna height multiplied by pinna width (MK/LM). Significant differences were observed for all features: Pinna width (**B**), Pinna length (**C**), Effective diameter (**D**), Nose to pinna distance (**E**), Inter pinna distance (**F**), Body length (**G**), Tail length (**H**), and Body mass (**I**). Peromyscus head image (**A**) was obtained from Rose Pest Solutions website and body/tail is from the OSU Collection of Vertebrates and is a preserved sample, not an animal that was measured in this current study. Image is presented only for demonstration of measurements.

Figure 4: Figure 4A and 4B show Auditory Brainstem response patterns of a female *P. leucopus* and a female *P. maniculatus* determined with clicks of different intensities, respectively. Hearing range was measured across frequency (1-64 kHz) for both *P. leucopus* and *P. maniculatus* (Figure 4C). No significant main effects of frequency between species were found. Unfilled blue circles represent *P. maniculatus* while filled pink squares represent *P. leucopus*.

Figure 5: Amplitudes of auditory brainstem responses wave I-IV. Data represent the response evoked by 90 dB SPL click stimuli between both species. No significant main effects of wave amplitude between species were found. Blue represents *P. maniculatus* while pink represents *P. leucopus*.

Figure 6: Latencies of auditory brainstem responses. Data represent latencies of ABR wave I-IV evoked responses by 90 dB SPL click stimulus between both species. No significant main effects of wave latency between species were found. Blue represents *P. maniculatus* while pink represents *P. leucopus*.

Figure 7: Average slope of latency-intensity function of waves I, and IV of ABRs (Pink = *P. leucopus* (n = 15), Blue = *P. maniculatus* (n = 11)).

Figure 8: Binaural hearing in wild *P. leucopus* (pink) and *P. maniculatus* (blue). Binaural amplitude and latency for the BIC with varying ITD between - 2 to + 2 ms in 0.5 ms steps were measured. No significant differences were observed between both species at BIC amplitudes. Significant differences were detected in BIC latencies between both species across all ITDs.

Table 1: Age was estimated based on body mass for each species based on published literature. Ages for *P. maniculatus* was describe as follows: Juveniles < 14 grams, subadults, between 14-17 grams, and adults, > 17 grams (Fairbairn, 1977). We inferred ages for *P. leucopus* as follow: Juveniles < 13 grams, subadults, between 13 – 18 grams, and adults > 18 grams (Cummings and Vessey, 1994). We did not make comparisons by ages due to limited sample sizes by age groups.

Table 2: Morphological characteristics features of *P. maniculatus* and *P. leucopus* of the Packsaddle wildlife management area (WMA), James Collin wildlife management area (WMA) and Payne County. Values presented represent the mean of different morphological features recorded, the degrees of freedom, F-statistic and p-value of morphological differences between species.